FERROELECTRIC CRYSTALS

by

FRANCO JONA

IBM Research Center

New York

and

G. SHIRANE

Westinghouse Research Laboratory

Pittsburgh

PERGAMON PRESS

OXFORD · LONDON · NEW YORK · PARIS

1962

CONTENTS

CHAPTER I

INTRODUCTION

1. General Features of Ferroelectric Crystals

THE MAIN problems which arise in the theory of dielectric crystals are concerned with the polarization that can be induced in such non-conducting materials by means of an externally applied electric field. The polarization values which can be measured in normal dielectrics upon application of experimentally attainable fields are usually small. Consequently, the effects that the polarization is expected to have on a number of physical properties of the crystals, such as the elastic, optical, thermal behavior, etc., are too small to be observed. Fortunately, a rather large, but yet limited, number of crystals exhibit polarization values which are many orders of magnitude larger than those observed in most dielectrics. The detailed study of some of these crystals has revealed many peculiar effects which are interesting not only from the point of view of dielectric theory, but also from that of crystallography, crystal-chemistry, thermodynamics, and, last but not least, practical applications in the field of electrical engineering.

It has become customary to call "ferroelectricity" the phenomenon exhibited by these crystals, and "ferroelectric" the crystals themselves. The reason for this denomination is historical and is due to a formal similarity of the ferroelectric phenomenon with that of ferromagnetism. The similarity is mainly phenomenological: just as ferromagnetic materials exhibit a spontaneous magnetization and hysteresis effects in the relationship between magnetization and magnetic field, ferroelectric crystals show a spontaneous electric polarization and hysteresis effects in the relation between dielectric displacement and electric field. This behavior is mostly observed in certain temperature regions delimited by transition (or Curie) points above which the crystals are no longer ferroelectric and show normal dielectric behavior.

Examples of typical ferroelectrics are: potassium di-hydrogen phosphate, KH_2PO_4, and a number of isomorphous phosphates and arsenates; barium titanate, $BaTiO_3$, and other isomorphous double oxides; Rochelle salt (sodium potassium tartrate tetrahydrate, $NaKC_4H_4O_6 \cdot 4H_2O$), and a few isomorphous crystals. The properties of these and other ferroelectrics will be discussed in detail in the following chapters. Reviews of these properties and the problems involved in the field of ferroelectricity are already available in the articles of Känzig (K 1) and Forsbergh (F 1) and in the book of Megaw (M 1). These authors follow different approaches in order to accomplish the task. Both Känzig and Forsbergh treat the problem of ferroelectricity in terms of the *properties* which characterize

the phenomenon. Megaw, on the other hand, presents her description of ferroelectricity in terms of *compounds*, rather than properties, and is particularly concerned with the crystallographic aspect of the problem. Our own approach, in the present treatment of the same problem, is to describe the properties of the various ferroelectric crystals individually, and to emphasize the *dielectric* character of the ferroelectric phenomenon as judged from the viewpoint of the solid-state physicist.

In order to describe the essential features of the ferroelectric phenomenon, let us introduce a model of a hypothetical ferroelectric crystal and see what kind

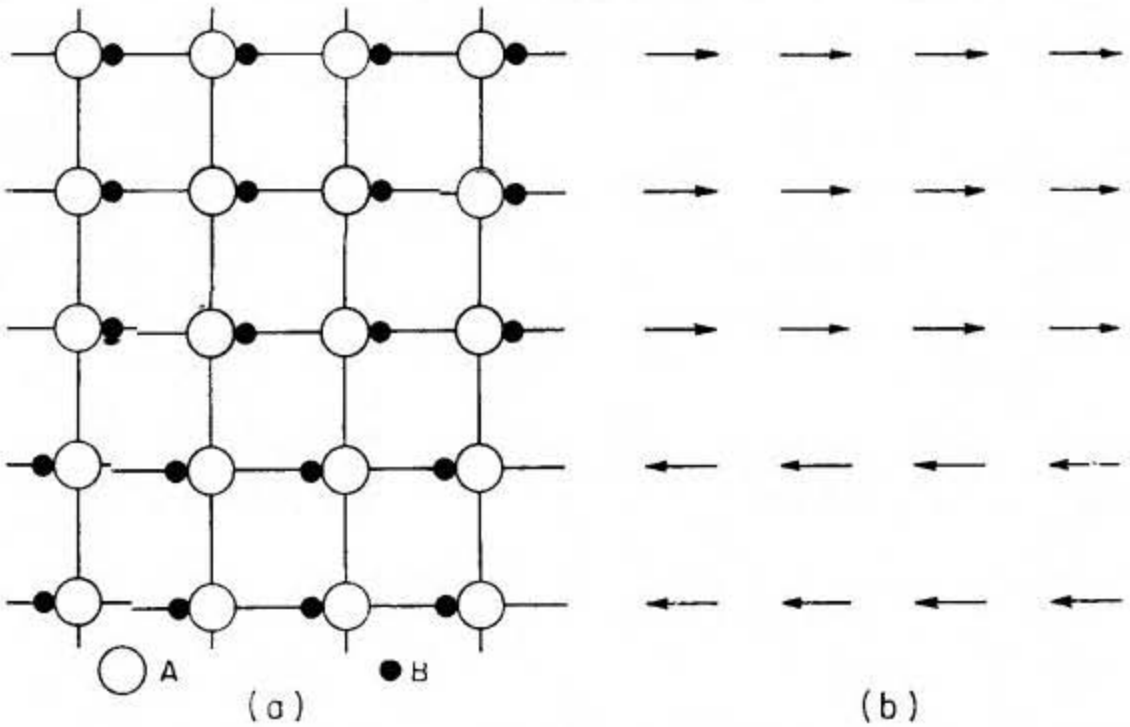

FIG. I-1. Schematic structure of a fictitious ferroelectric crystal.

of dielectric behavior it would show. The model, which has, of course, no general validity and is extremely oversimplified, is that of a two-dimensional crystal having the chemical formula AB and a fictitious structure depicted in Fig. I-1 (a).

The A ions, which we will assume to carry a negative charge, are located on the lattice points of a simple square net. The B ions, carrying a positive charge, are located on the horizontal lines joining the A ions; their equilibrium positions are such that they always lie closer to one of the two adjacent A ions than to the other. Such a situation is possible if the potential between two adjacent A ions is of the type sketched in Fig. I-2 (a): there are two equilibrium positions, corresponding to the same minimum value of the energy, for a B ion on the line joining two A ions. The B ions can jump from one equilibrium position to the other but in order to do so they must be provided with the energy necessary to overcome the energy barrier ΔE.

Suppose now that, at a given temperature T, all B ions are closer to their A partners on the left. We can visualize every group AB as an electric dipole and the structure can then be schematically represented by an assembly of dipoles

pointing all in the same direction, as in the three upper rows of Fig. I-1 (b). We say that the crystal is *spontaneously polarized*: the *spontaneous polarization* is measured in terms of dipole moment per unit volume, or, with reference to the charges induced on the surfaces perpendicular to the polarization, in terms

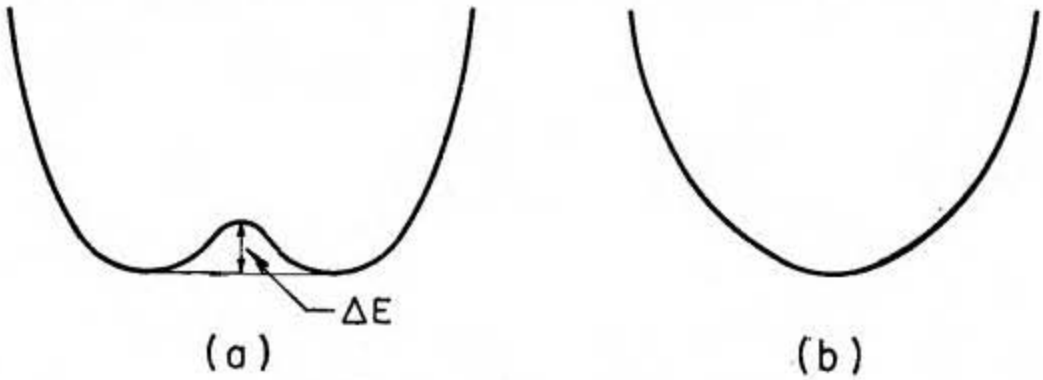

FIG. I-2. Schematic potential wells.

of charge per unit area. The crystals having a spontaneous polarization are called *pyroelectric* (see Section 3) and the direction of the spontaneous polarization is called the *polar axis*.

Alignment of the electric dipoles may extend only over a region of the crystal, while in another region the direction of the spontaneous polarization may be reversed, as in the lower portion of Fig. I-1 (b). Such regions of uniform polarization are called *domains*, a term borrowed again from ferromagnetism. We are going to see in the following that energy considerations require the formation of domains.

Suppose now that we apply an electric d.c. field in the horizontal direction of Fig. I-1. The dipoles which are already oriented in the direction of the field will remain so aligned, but those which are oriented in the direction opposite (antiparallel) to the field will show a tendency to reverse their orientation. If the applied field is sufficiently large, the B ions of our model will be able to overcome the barrier ΔE, and in so doing will cause the corresponding dipole to flip (or switch) over into the direction of the field. This phenomenon of polarization reversal takes place by way of a nucleation process and domain-wall motions. The question which immediately arises is this: how does the process of polarization reversal affect the relation between polarization P and applied electric field E?

Suppose that our crystal is initially composite of an equal number of positive and negative domains (i.e. domains oriented to the right and domains oriented to the left), which means that the overall polarization of the crystal is equal to zero. If we first apply a small electric field directed say, in the positive direction, we will have only a linear relationship between P and E because the field is not large enough to switch any of the domains and the crystal will behave like a normal dielectric! In the plot of P vs. E, shown schematically in Fig. I-3, we obtain the portion OA of the curve. If we increase the electric field strength, a number of the negative domains will switch over in the positive direction and

the polarization will increase rapidly (portion AB), until we reach a state in which *all* the domains are aligned in the positive direction: this is a state of saturation (portion BC) and the crystal consists now of a single domain.

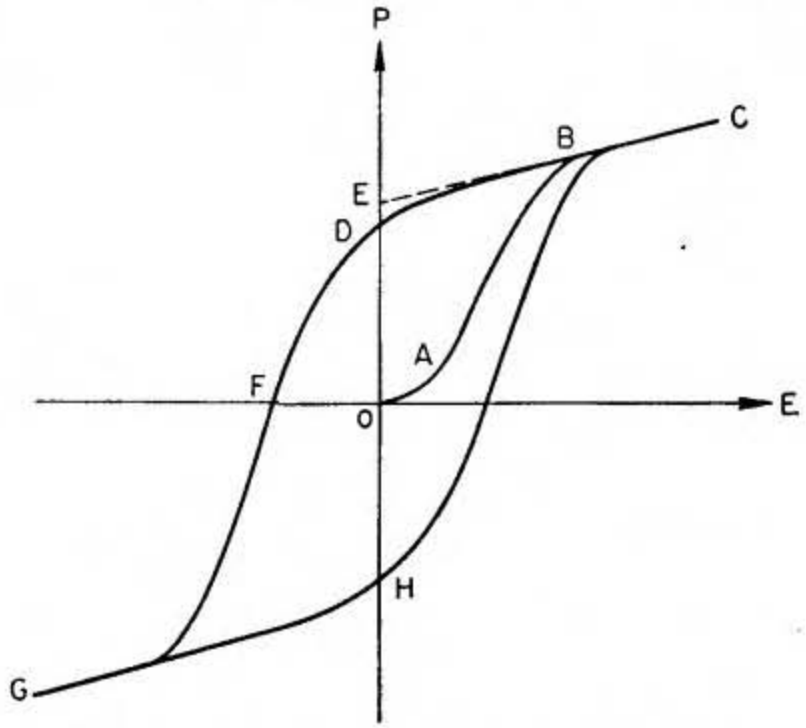

FIG. I-3. Ferroelectric hysteresis loop (schematic).

If we now decrease the field strength, the polarization will generally not return to zero but rather follow the path CD of Fig. I-3. When the field is reduced to zero, some of the domains will remain aligned in the positive direction and the crystal will exhibit a *remenant polarization* $P_r(OD)$. The extrapolation of the linear portion BC of the curve back to the polarization axis represents the value of the *spontaneous polarization* $P_s(OE)$.

In order to annihilate the overall polarization of the crystal, we find it necessary to apply an electric field in the opposite (negative) direction. The value of the field required to reduce P to zero (OF) is called the *coercive field* E_c. Further increase of the field in the negative direction will, of course, cause complete alignment of the dipoles in this direction (FG), and the cycle can be completed by reversing the field direction once again (GHC).

The relation between P and E is thus represented by a *hysteresis loop* ($CDGHC$), which is the most important characteristic of a ferroelectric crystal. The essential feature of a ferroelectric is thus *not* the fact that it has a spontaneous polarization, but rather the fact that this spontaneous polarization can be reversed by means of an electric field. It may be noted that, owing to the relation between dielectric displacement D, electric field E, and polarization P,

$$D = E + 4\pi P,$$

the relation between D and E is also characterized by a hysteresis curve. The analogy with the well-known ferromagnetic hysteresis loop representing the relation between magnetic induction B and magnetic field H is obvious.

Ferroelectric hysteresis loops can be observed very easily on the screen of an oscilloscope by inserting the crystal in a simple circuit first described by Sawyer and Tower (S 1) and using an a.c. field (generally 60 c/s). The circuit is depicted schematically in Fig. I-4: the voltage lying across the crystal C_x is put on the horizontal plates of the oscilloscope, thus plotting on the horizontal axis a quantity which is proportional to the field lying across the crystal. The linear capacitor

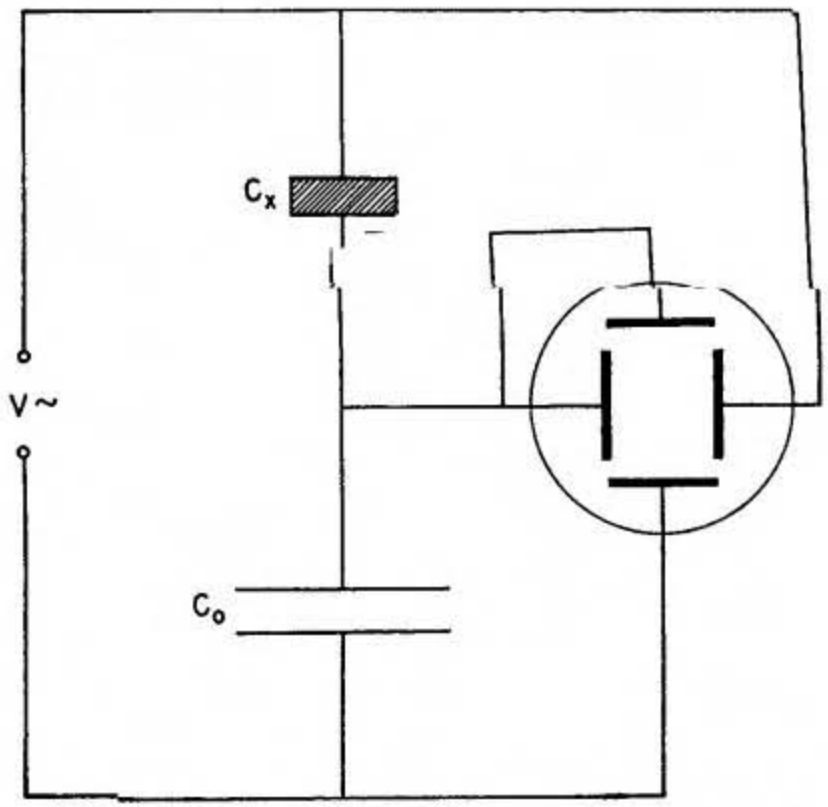

FIG. I-4. Schematic circuit for the observation of ferroelectric hysteresis loops (according to Sawyer and Tower (S 1)).

C_0 is connected in series with the crystal C_x and the voltage lying across C_0 is therefore proportional to the polarization of the crystal C_x. This voltage is laid across the vertical plates of the oscilloscope. The Sawyer and Tower circuit allows not only the display of the hysteresis loop on the scope screen, but also the measurement of important quantities such as the spontaneous polarization P_s and the coercive field E_c.

We have mentioned above that the most important property of a ferroelectric is the reversibility of its spontaneous polarization. The fact that an applied field can cause the polarization to alter its orientation has some important consequences. In the first place, it means that the shift of the B ions is small, and this small relative shift turns the crystal into its electrical twin. It is not illogical to expect, then, that if the energy barrier ΔE (Fig. I-2a) is so low as to be accessible with the help of an electric field, then it may also be affected by other factors, such as temperature changes.

With increasing temperature, the thermal motion of the atoms in the lattice will increase to such an extent that the B ions of our fictitious crystal may be

able to overcome the energy barrier ΔE without the help of an external field, and may therefore jump from one equilibrium position to the other.

Another possibility is that the shape of the potential curve between adjacent A ions changes to the point of becoming as indicated schematically in Fig. I-2(b). In the latter case, there is only one equilibrium position possible for the B ions, i.e. midway between two A ions. In the former case, the statistical distribution of the B ions will be symmetrical with respect to the A ions. The result is the same: our crystal is no longer polar, and will behave rather as a normal dielectric material.

The temperature at which such a transition from the polar into the non-polar state occurs is often referred to as *Curie temperature* (or *Curie point*), again in analogy with ferromagnetism. Almost all ferroelectric crystals known to date have a Curie point, and those which do not have it simply decompose before such a temperature is reached.*

Another consequence of the small atomic shifts occurring in ferroelectric crystals is the behaviour of the dielectric constant of these crystals as a function of temperature. The dielectric constant is normally defined as the derivative of the dielectric displacement D with respect to the field E. Similarly, the derivative of polarization P with respect to field E is usually defined as the dielectric susceptibility k. Owing to the well-known relationship between D, E and P:

$$D = E + 4\pi P,$$

the dielectric constant ε is related to the dielectric susceptibility k, in the c.g.s. system, through the equation

$$\varepsilon = 1 + 4\pi k.$$

This definition of the dielectric constant is significant and consistent for normal dielectrics in which the relationship between D and E is linear up to large values of E. In the case of ferroelectric crystals, ε must be defined more precisely, owing to the more complicated relation between D and E (Fig. I-3). For our purposes, we are going to define the dielectric constant ε as the slope of the D–E curve at the origin:

$$\left(\frac{\partial D}{\partial E}\right)_{E=0}$$

and we are going to measure it with very small a.c. fields, so as not to reverse any domains.

As the potential curve between two adjacent A ions of our crystal changes with temperature, the polarizability of the B ions moving within such a curve will change accordingly. It is thus to be expected that the dielectric constant ε

* It has become customary, in many publications, to refer to the phase above the Curie point as to the "paraelectric" phase; ferroelectric crystals are, therefore, often said to become "paraelectric" above their Curie temperature. This term originates again from the formal similarity with the behaviour of a ferromagnetic crystal becoming paramagnetic above its transition point. We prefer, however, to refrain from usage of such a term, and we will refer to the state of a ferroelectric crystal above its Curie temperature as the "non-polar" state.

will exhibit some kind of anomaly at the transition temperature. Generally, any kind of phase transition in dielectrics is accompanied by an anomaly of the dielectric constant; a ferroelectric transition, being generally a transition from a polar into a non-polar phase, is no exception to this rule. In some ferroelectrics, the temperature dependence of the dielectric constant above the transition temperature can be described fairly accurately by a simple law, called the *Curie–Weiss law* from its ferromagnetic analog:

$$\varepsilon = \varepsilon_0 + \frac{C}{T - T_0}$$

where the temperature-independent part ε_0 can often be neglected, C is the *Curie constant* and T_0 the *Curie–Weiss temperature*. It is advisable, in general, to distinguish between this Curie–Weiss temperature T_0 and the Curie (or transition) temperature T_c.

In the vicinity of the Curie–Weiss temperature, the dielectric constant becomes very large, and the relationship between dielectric constant and susceptibility can be approximated by

$$\frac{\varepsilon}{4\pi} \cong k .$$

We are going to see in the following that in certain ferroelectrics (which undergo a transition of the second order) the Curie–Weiss temperature T_0 practically coincides with the transition temperature T_c, but in others (which undergo a transition of the first order) it does not. It must be emphasized that a hyperbolic dependence of the dielectric constant on temperature, such as the Curie–Weiss law, is by no means a necessary condition for a ferroelectric transition, as it was customary to believe in the early stages of ferroelectric research. The fact that in some ferroelectrics the anomaly of the dielectric constant is large and the Curie–Weiss law is obeyed may simply mean that the co-operative phenomeno. leading to ferroelectricity has a dielectric origin in these crystals, while in others it may have a different character. As we are going to see in the following, a number of characteristic quantities other than the dielectric constant may exhibit anomalies at the transition temperature. This point will be better discussed when we treat specific cases.

2. Spontaneous Polarization

There are a number of fundamental inaccuracies in the description of the model which we have introduced in the preceding section, in spite of the fact that it helps to account for the general features of ferroelectric crystals.

In the first place, we have arbitrarily picked out pairs of atoms and attributed to each of them a dipole moment, defined, as is customary, as the product of charge and separation. This procedure is definitely not legitimate in a real structure. It is true that in a ferroelectric crystal every unit cell carries a dipole moment, but we cannot generally attribute this dipole moment to a specific pair of atoms in the unit cell without making arbitrary assumptions about the interatomic forces.

All we can say is that, given a charge distribution $\varrho(r)$ within a given crystal, the electric moment with respect to an *arbitrary* origin,

$$\iiint \varrho(\boldsymbol{r}) \cdot \boldsymbol{r} \cdot \mathrm{d}v,$$

is different from zero and the value of this volume integral is independent of the choice of the origin. To attribute this electric moment to a given pair of atoms would imply that this atomic pair is held together by forces which are stronger than those which bound it to the rest of the structure. This implication is incorrect, because the two atoms which we have picked out are bound to their neighbors by the same forces as those that bind them to each other.

A second important point which does not appear clear in the simple model introduced before is that the dipole moment of each unit cell does not consist only of ionic charges. Eventually, charge separation may occur through the distortion of the electronic cloud of a given atom. In other words, the charge distribution $\varrho(r)$ within the crystal involves not only the ionic but also the electronic charge. Although a distinction between these two contributions to the electric moment is experimentally quite difficult, the concepts of ionic and electronic polarization have been introduced often in the literature. It may be pointed out that these concepts constitute a very important difference between ferroelectricity and ferromagnetism. In ferroelectric crystals, the dipoles are imbedded in a highly polarizable medium ("background"), whose polarizability is temperature dependent, while in ferromagnetic crystals the magnetic moments due to the spin cannot be influenced by the "background".

It should also be pointed out that the simple model introduced in Section 1 is mainly concerned with phenomenological consequences of a spontaneous polarization which is somehow assumed to be already existing within the crystal. We have, in other words, approached the problem of ferroelectricity from the point of view which assumes an already *polarized* state. What we should also do, however, is to follow the opposite approach, starting from the *unpolarized* state, and inquire about the interatomic forces which are at work to bring about spontaneous polarization in a crystal lattice. This problem is of fundamental importance in the general theory of dielectrics, and the reader may be referred, for the details of the following arguments, to the textbooks of Böttcher (B 1), Brown (B 2), Dekker (D 1), Fröhlich (F 2), Kittel (K 2), or Smyth (S 2).

Given a particular type of atom in a substance, we define the polarizability α of such an atom as the ratio between the dipole moment (permanent or induced) of the atom and the electric field acting upon it:

$$\alpha = \mu / F.$$

The field F is generally given by Lorentz's formula for the internal field acting on a dipole located in a lattice of *equal* dipoles with *cubic* symmetry:

$$F = E + \frac{4\pi}{3} P.$$

Straightforward use of this formula leads to the well-known Clausius–Mosotti equation for the dielectric constant ε:

$$\frac{\varepsilon - 1}{\varepsilon + 2} = \frac{4\pi}{3} N\alpha,$$

where N is the number of the dipoles per unit volume. The above equation can be re-written in the following form:

$$\varepsilon = \frac{1 + (8\pi/3) N\alpha}{1 - (4\pi/3) N\alpha}.$$

From this, it follows that the dielectric constant ε becomes infinite, corresponding to a finite polarization for zero applied field, when

$$N\alpha = \frac{3}{4\pi}.$$

Putting, for example,

$$1 - \frac{4\pi}{3} N\alpha = \frac{3}{C}(T - T_0),$$

we immediately obtain a Curie–Weiss law for the dielectric constant

$$\varepsilon \cong \frac{C}{T - T_0}$$

in agreement with the observed temperature dependence of the dielectric constant of some ferroelectrics above the Curie temperature.

Thus, it is seen that a simple assumption about the temperature dependence of the product $N\alpha$, combined with Lorentz's internal-field formula leads easily to a ferroelectric transition and a Curie–Weiss law. However, the shortcomings of this theory appear especially obvious when it is applied to polar liquids: when numerical values are inserted, it turns out that liquids such as water should be spontaneously polarized at room temperature, an obviously absurd result which has been called the "$4\pi/3$ catastrophe". This catastrophe occurs in the case of fields produced by permanent dipoles, and can only be avoided by using modified internal-field formulae derived by Onsager, Kirkwood, Oster and Fröhlich (see e.g., Refs. (B 1), (B 2), (F 2), (J 1), (S 1)). In the case of induced moments, the theory can be used, provided the proper correction of the Lorentz's formula for the internal field is applied, as was shown by Slater in the case of ferroelectric barium titanate (see Chapter IV).

It is, however, generally true that consideration of the long-range forces characterized by Lorentz's formula is insufficient to explain the onset of spontaneous polarization in a given crystal lattice. This is not only due to the fact that the Lorentz formula was derived for a lattice of equal dipoles with cubic symmetry and, as such, represents merely a first approximation. In some cases, the consideration of short-range coupling is necessary; in fact it may be sufficient to explain the occurrence of a ferroelectric transition, although it may not suffice to reproduce the exact character of the transition. A typical example of this is Slater's theory for KH_2PO_4. (See Chapter III.)

3. Crystallographic Considerations and Definition of a Ferroelectric

It is well known that any one crystal can be classified in one or another of thirty-two crystal classes (point groups) according to the symmetry elements which it possesses. A study of these thirty-two classes reveals that eleven of them are characterized by the existence of a center of symmetry: they are thus called *centrosymmetric*. A centrosymmetric crystal can of course possess no polar properties. If, for example, we apply a uniform stress to such a crystal, we will indeed cause a small displacement of the charges within the lattice, but the existence of a center of symmetry will bring about a compensation of the relative displacements. If we apply an electric field to a centrosymmetric crystal, we will indeed change its shape, but the strain will remain unchanged if we reverse the direction of the electric field. In other words, the strain is proportional to the square of the applied field: the effect is quadratic. This is the effect called *electrostriction*, which occurs actually in *all* substances, whether crystalline or amorphous, solid or fluid.

The remaining twenty-one crystal classes do not have a center of symmetry; they are non-centric. The absence of a center of symmetry makes it possible for crystals in these classes to have one or more polar axes and thus to show vectorial or tensorial properties. With one exception, all classes devoid of a center of symmetry exhibit the *piezoelectric effect*. The single exception is the cubic class 432 which, although without a center of symmetry, nevertheless has other symmetry elements that combine to exclude the piezoelectric activity. Piezoelectricity is the property of a crystal to exhibit electric polarity when subject to stress. The piezoelectric effect is a *linear* effect; application of pressure to a piezoelectric crystal plate between two electrodes causes a charge to flow in a certain direction through a measuring circuit. If the pressure is replaced by a tension, the charge will flow in the opposite direction. Also, if we apply an electric field to the crystal plate, it will be stretched; if we reverse the field direction, it will be compressed. This is the converse piezoelectric effect.

Out of the twenty piezoelectric classes, ten are characterized by the fact that they have a *unique* polar axis, i.e. an axis which shows properties at one end different from those at the other. Crystals in these classes are called *polar* because they are spontaneously polarized. Generally, this spontaneous polarization cannot be detected by charges on the surface of the crystal because these charges have been compensated through external or internal conductivity, or by twinning. The value of the spontaneous polarization, however, is dependent on temperature; thus, if the temperature of the crystal is altered a change in the polarization occurs and electric charges can be observed on those crystal faces which are perpendicular to the polar axis. This is the *pyroelectric* effect. The ten crystal classes which have a unique polar axis are also called pyroelectric classes.

It follows from the discussion in Section 1 that the ferroelectric crystals belong to the pyroelectric family. They constitute only that part of it, however, for which the direction of the spontaneous polarization can be reversed by appli-

cation of an electric field. It is thus a *necessary* condition for a ferroelectric crystal to belong to any one of the ten polar classes (in its ferroelectric phase) but not a sufficient condition, as reversibility of the polarity must also occur. We can thus *define* a *ferroelectric* crystal as a *pyroelectric crystal with reversible polarization*.

This definition brings about an interesting difference between ferroelectricity and ferromagnetism. In the case of ferromagnetism, whenever the moments are spontaneously aligned they can also be reversed by means of an external field. Thus, the magnetic phenomenon is interesting *because* the moments are spontaneously aligned. The phenomenon of ferroelectricity, on the other hand, is interesting only when the moments are loosely aligned, i.e. when the interactions are so delicately balanced as to allow reversal of the spontaneous polarization.

It should be noted that the existence of a unique polar axis in the point group symmetry of a given crystal can, in principle, be established, e.g. by means of *X*-rays, but its reversibility can be established only by dielectric measurements.

4. Classification of Ferroelectrics

For a number of years, the phenomenon of ferroelectricity was known to occur in a rather limited number of crystals, viz. Rochelle salt, potassium di-hydrogen phosphate, barium titanate and a number of compounds isomorphous with these crystals. At this stage, various classifications of the ferroelectric materials were proposed, in order to facilitate the treatment of their properties. In recent years, however, owing particularly to the efforts of Matthias, Pepinsky, Smolenskii and co-workers, the number of ferroelectric crystals known has increased to a point where ferroelectricity appears to be a somewhat more common phenomenon than had been thought for a long time, and a satisfactory classification of all the materials has become very difficult.

Table I-1 provides a partial list of ferroelectric crystals arranged approximately in chronological order of their discovery. It is seen that, from the chemical point of view, representative ferroelectrics can be found among the tartrates, phosphates, arsenates, double oxides, sulfates, borates, propionates, nitrates, nitrites, etc. The symmetries of the non-polar phases vary from cubic to tetragonal, orthorhombic and monoclinic, and the Curie temperatures range from approximately 10 °K, for potassium tantalate, to about 840 °K for lead metaniobate. The values of the spontaneous polarization vary from the order of 10^{-7} C/cm^2 to about 10^{-4} C/cm^2. It may be interesting to point out in this respect that in normal dielectrics, such as, for example, the alkali halides, such high values of the polarization could theoretically be attained only with electric fields of the order of from 10^5 to 10^8 V/cm.

The following is a summary of the criteria according to which various classifications of the ferroelectric materials have been or could be proposed:

(i) Crystal–chemical classification. According to this classification, the ferroelectric compounds may be divided into two groups. The first group comprises hydrogen-bonded crystals, such as KH_2PO_4, Rochelle salt, tri-glycine sulfate,

etc. The second group includes the double oxides, such as $BaTiO_3$, $KNbO_3$, $Cd_2Nb_2O_7$, $PbNb_2O_6$, $PbTa_2O_6$, etc.

(ii) Classification according to the number of directions allowed to the spontaneous polarization. Again, ferroelectric materials can be divided into two groups; a group involving a single axis of the spontaneous polarization, in which

TABLE I-1. PARTIAL LIST OF FERROELECTRIC CRYSTALS

(The values of the spontaneous polarization reported in the third column are either the room-temperature or the maximum values)

Name and chemical formula	Curie temperature (°C)	Spontaneous polarization (10^{-6} C/cm^2)	Year in which reported
Rochelle salt $NaKC_4H_4O_6 \cdot 4H_2O$	+ 23	0.25	1921
Lithium ammonium tartrate $Li(NH_4)C_4H_4O_6 \cdot H_2O$	− 170	0.20	1951
Potassium di-hydrogen phosphate KH_2PO_4	− 150	4.7	1935
Potassium di-deuterium phosphate KD_2PO_4	− 60	5.5	1942
Potassium di-hydrogen arsenate KH_2AsO_4	− 177	5.0	1938
Barium titanate $BaTiO_3$	− 120	26.0	1945
Lead titanate $PbTiO_3$	− 490	>50	1950
Potassium niobat $KNbO_3$	− 415	30	1951
Potassium tantalate $KTaO_3$	− 260	?	1951
Cadmium (pyro) niobate $Cd_2Nb_2O_7$	− 85	~10	1952
Lead (meta) niobate $PbNb_2O_6$	+ 570	?	1953
Guanidinium aluminium sulfate hexahydrate $C(NH_2)_3Al(SO_4)_2 \cdot 6H_2O$	None	0.35	1955
Methylammonium aluminium alum $CH_3NH_3Al(SO_4)_2 \cdot 12H_2O$	− 96	1.0	1956
Ammonium sulfate $(NH_4)_2SO_4$	− 50	0.25	1956
Tri-glycine sulfate $(NH_2CH_2COOH)_3 \cdot H_2SO_4$	+ 49	2.8	1956
Colemanite $CaB_3O_4(OH)_3 \cdot H_2O$	− 7	0.65	1956
Dicalcium strontium propionate $Ca_2Sr(CH_3CH_2COO)_6$	+ 8	0.3	1957
Lithium acid selenite $LiH_3(SeO_3)_2$	None	10.0	1959
Sodium nitrite $NaNO_2$	+ 160	7.0	1958

we put the ferroelectrics which can polarize only along one axis, such as Rochelle salt, KH_2PO_4, colemanite, $PbTa_2O_6$, etc., and a group comprising crystals which can polarize along several axes that are crystallographically equivalent in the non-polar phase, such as $BaTiO_3$, $Cd_2Nb_2O_7$, the ferroelectric alums, etc. This classification may be particularly useful for the study of ferroelectric domains.

(iii) Classification according to the existence or lack of a center of symmetry in the point group of the non-polar phase. A first group of ferroelectrics is characterized by a non-polar phase which is piezoelectric (non-centrosymmetrical), such as Rochelle salt, KH_2PO_4, and isomorphous compounds. A second group of ferroelectrics is characterized by a centrosymmetrical non-polar phase, such as $BaTiO_3$, $Cd_2Nb_2O_7$, tri-glycine sulfate, etc. This classification may be particularly useful for the thermodynamic treatment of the ferroelectric transitions.

(iv) Classification according to the nature of the phase change occurring at the Curie point. A first group of ferroelectrics undergo a transition of the order–disorder type, as KH_2PO_4, tri-glycine sulfate and probably some of the alums. A second group of compounds undergo a transition of the displacive type, such as that of barium titanate and most of the double oxide ferroelectrics. This classification is practically equivalent to that done on the basis of the existence of permanent or induced dipoles in the non-polar phases of the crystals. A characterization of the nature of the phase change in the sense mentioned above (order–disorder vs. displacive) can, in principle, be met on the basis of accurate structural investigations. In some cases, however, this information is already available from the results of dielectric investigations.

If we examine the temperature dependence of the dielectric constant, or in other words, the value of the Curie constant C appearing in the Curie–Weiss law, we see that the various ferroelectrics can be divided into two main groups (see Table I-2). Compounds in the first group have Curie constants of the order of 10^3. It can be shown that this order of magnitude is to be expected for a substance containing a number of similar dipoles, each of which has two positions of equilibrium corresponding to opposite orientations of the dipole. This dipole model is practically equivalent to that of an ion moving in the type of potential shown in Fig. I-2(a). The dielectric constant ε of such a model assumes the following form (D 2):

$$\varepsilon = \frac{4\pi}{\gamma} \frac{T_0}{T - T_0},$$

where γ is the Lorentz factor appearing in the Lorentz internal-field formula $F = E + \gamma P$, and T_0 is the Curie–Weiss temperature. The factor γ will depend on the particular atomic structure but will be of the order of $4\pi/3$. Thus, we can write for the dielectric constant:

$$\varepsilon \cong \frac{3T_0}{T - T_0},$$

TABLE I-2. CURIE CONSTANTS C, DEFINED FROM THE CURIE–WEISS LAW $\varepsilon = \frac{C}{T - T_0}$, FOR VARIOUS FERROELECTRICS

Substance	C (degrees)
Rochelle salt	2.2×10^3
KH_2PO_4	3.3×10^3
Colemanite	0.5×10^3
Tri-glycine sulfate	3.2×10^3
Methylammonium aluminium alum	1.0×10^3
$NaNO_2$	5.0×10^3
$BaTiO_3$	1.5×10^5
$KNbO_3$	2.0×10^5
$Cd_2Nb_2O_7$	1×10^5
$PbNb_2O_6$	3×10^5

implying that the Curie constant C is of the order of $3T_0$, i.e. for $T_0 \sim 300$ °K, of the order of 10^3.

The second group of ferroelectrics shown in Table I-2 exhibit Curie constants of the order of 10^5. This can be explained by assuming that the substances in this group contain, say, N oscillating ions per unit volume and that each ion produces an electric moment ex when it is displaced a distance x from its normal equilibrium position. Expressing the energy of an ion relative to its equilibrium position in the form $ax^2 + bx^4$, Devonshire (D 2) has shown that the dielectric constant assumes the form:

$$\varepsilon = \frac{4\pi Ne^2}{6k} \frac{a}{b} \frac{1}{T - T_0},$$

where k is Boltzmann's constant. Thus, the temperature dependence of the dielectric constant depends on the anharmonic term bx^4 in the energy of an ion. This corresponds to the model of an ion moving in a potential of the type shown in Fig. I-2(b). This equation shows that if the coefficient b is small, the temperature dependence of ε is small and hence the Curie constant will be large.

Clearly, any intermediate type of potential field between the two extreme cases shown in Fig. I-2 is possible for the non-polar phase of the ferroelectrics, but it is significant that most of the ferroelectrics known belong rather to either one of these extreme models as shown in Table I-2. A classification made on this basis may, therefore, be useful in discussing the types of ferroelectric transitions.

It is evident that the four classifications described above do not coincide with each other. Each one is useful only when discussing a particular aspect of the ferroelectric phenomenon, but a consistent classification of all ferroelectrics appears hardly possible at the present stage. It is thus more appropriate to restrain from making any such classification at this stage, but to proceed with the detailed description of the phenomenological and structural characteristics

of the cases known. Accordingly, the phenomenological and model theories will be discussed, for several of the most typical ferroelectrics, in the corresponding chapters devoted to the particular crystals for which the theories were developed.

In order to supplement this approach we have provided in Appendix II a concise analytical index in table form. In this table we have listed the numbers of chapters and sections where the individual topics are treated somewhat extensively. This table is by no means complete; it is hoped, however, that it may help the reader interested in comparisons among various ferroelectrics.

5. Introduction to the Thermodynamic Theory of Crystals

Because the general features of the phenomenological behavior of most ferroelectrics are the same, it is convenient to present first an introduction to the thermodynamic theory of the crystalline state. The value of such a theory is significant in disclosing what thermodynamic properties are needed in order to account for the experimental facts, and therefore what features are to be looked for in some future successful model. The development of the following thermodynamic treatment is due to Mueller (M 2), Cady (C 1), and Devonshire (D 2).

A crystal, whether ferroelectric or not, is a thermodynamic system whose equilibrium state can be completely specified by the values of a number of variables. The internal energy of the system can, in fact, be expressed as a function of the mechanical and electrical stresses X and E, respectively, or the mechanical and electrical strains x and P, respectively, in addition to temperature and entropy. Of the four variables X, E, x and P we can choose two as independent, the other two as dependent variables, depending on what we have in mind. Experimentally, for example, it is generally easier to vary the external stresses X and the applied electric fields E, so that it is logical to assume the strains x and the polarization P as dependent variables. For theoretical considerations, on the other hand, the opposite is true. Whatever the choice, we must realize that, as P and E are vectors (three components), and x and X tensors (six components), the energy state of our crystal is specified when we know the values of ten variables (these nine components plus the temperature). It is a basic postulate of thermodynamics that a unique function of these ten variables exists, which is called the free energy function; we are attempting to present a simple analytical expression of this function.

Suppose that we consider the strains x and the polarization P as independent variables. We can always expand the (unknown) free energy function in powers and products of the components of strain and polarization. We can then see whether this power series converges and determine how many terms we need in order to describe the electromechanical behavior of the crystal. We assume, for simplicity, that the free energy of the unstrained, unpolarized crystal is equal to zero; we can refer the strains to the equilibrium configuration of the crystal in the absence of stresses. Insofar as the strains are small, as is usually the case, only quadratic terms need be retained, which, in elastic treatments, amounts to

the acceptance of Hook's law. However, in view of the application of the thermodynamic theory to ferroelectric crystals, in which the polarization assumes unusually large values, we are going to include terms in higher orders of the polarization components. The effect of temperature is taken into account by assuming that the coefficients of the power series are functions of temperature.

We thus postulate the following expression for the free energy of the crystal in terms of strains and polarization:

$$\begin{aligned} A(x, P) = {} & \tfrac{1}{2}\sum_1^3 \chi_{ij} P_i P_j + \tfrac{1}{3}\sum_1^3 \omega^x_{ijk} P_i P_j P_k + \\ & + \tfrac{1}{4}\sum_1^3 \xi^x_{ijkl} P_i P_j P_k P_l + \tfrac{1}{5}\sum_1^3 \psi^x_{ijklm} P_i P_j P_k P_l P_m + \\ & + \tfrac{1}{6}\sum_1^3 \zeta^x_{ijklmn} P_i P_j P_k P_l P_m P_n + \\ & + \tfrac{1}{2}\sum_1^3 c^P_{ijkl} x_{ij} x_{kl} + \\ & + \sum_1^3 a_{ijk} x_{ij} P_k + \tfrac{1}{2}\sum_1^3 q_{ijkl} x_{ij} P_k P_l + \cdots \end{aligned} \qquad \text{(I-1)}$$

where the summations are carried out for all possible combinations of the subscripts running from 1 to 3 (according to the usual convention that, for example, $P_x = P_1$, $P_y = P_2$, $P_z = P_3$). The superscripts of the coefficients are necessary to specify the conditions under which such coefficients are observed: the superscript x means that the coefficient is observed at constant strain, the superscript P that it is observed at constant polarization. Some of the coefficients of the free energy expansion (I-1) have a familiar physical meaning. χ_{ij} represents the reciprocal dielectric susceptibility of the unpolarized crystal, c_{ijkl} the tensor of the elastic constants, a_{ijk} that of the piezoelectric constants, q_{ijkl} that of the electrostrictive constants.

It may be helpful to recall that the piezoelectric constants a_{ijk} form a third-rank tensor, while the elastic constants c_{ijkl} and the electrostrictive constants q_{ijkl} are fourth-rank tensors. In this notation, there are twenty-seven components of the piezoelectric coefficients and eighty-one components of the elastic constants (see, e.g., the book of Nye (N 1) and the article of Smith (S 3)). The full tensor notation is useful when one wants to display the true character, and particularly the transformation properties, of the coefficient involved. But for calculations in particular problems it is advantageous to reduce the number of suffixes as much as possible, i.e. to use the matrix notation. In the case of a third-rank tensor, the first suffix is maintained, but the second and third suffixes in the full tensor notation are replaced in the new notation by a single suffix running from 1 to 6 as follows:

tensor notation	11	22	33	23,32	31,13	12,21,
matrix notation	1	2	3	4	5	6 .

In the case of a fourth-rank tensor, the first two suffixes are abbreviated into a single one running from 1 to 6, the last two are abbreviated in the same way, according to the same scheme given above. The same formal change is made for the stress and strain components in order to reduce them from the two-suffixes to the one-suffix notation.* It must be remembered, however, that in spite of their appearance, with two suffixes, the piezoelectric and elastic constants do not transform like the components of a second-rank tensor. With the matrix notation, in the most general case (triclinic symmetry), there are six dielectric, twenty-one elastic, eighteen piezoelectric and thirty-six electrostrictive terms, but consideration of the symmetry elements represented in the point group of the crystal reduces the number of the non-zero coefficients.

For a crystal belonging to a centrosymmetrical class, the terms involving odd powers of the polarization vanish, as well as the piezoelectric term. In the case of a piezoelectric crystal, we may, in the first approximation, neglect the electrostrictive term.

In Eq. (I-1) we have not included, for simplicity, the terms which describe the thermal, thermoelastic and pyroelectric properties of the crystal. Moreover, it should be noticed that, in general, the derivatives of the above free-energy function with respect to the strain x and the polarization P are *not* the externally applied stress X and field E, respectively, as in the usual thermodynamic formalism. The derivative with respect to x is rather the *total* stress, consisting of two parts: (1) the externally applied stress that would produce the prescribed strain if $P = 0$; (2) the stress caused piezoelectrically by the polarization P (C 1). Similarly, the derivative of $A(x, P)$ with respect to P is not the externally applied field, but rather the field that would produce, in a clamped crystal, the same total polarization which is given by the prescribed values of P and x. If the strain $x = 0$, and there is no spontaneous polarization, then $[\partial A(x, P)/\partial P]_{x=0}$ is equal to the externally applied field; if the polarization $P = 0$, then $[\partial A(x, P)/\partial P]_{P=0}$ is the field that would cause, in a clamped crystal, the polarization due to x (C 1).

We first want to consider the case of a piezoelectric, but not ferroelectric, crystal. We therefore neglect the terms of order higher than the second in P, and the electrostrictive term. Also, we eliminate, for simplicity, the suffixes and the summation signs and write the free energy formally in the following way:

$$A(x, P) = \tfrac{1}{2} c^P x^2 + \tfrac{1}{2} \chi^x P^2 + a P x. \tag{I-2a}$$

Similarly, we can write the free energy in terms of stress X and polarization P thus:

$$A(X, P) = \tfrac{1}{2} s^P X^2 + \tfrac{1}{2} \chi^X P^2 - b P X, \tag{I-2b}$$

* The same convention applies of course to the piezoelectric and elastic coefficients to be introduced later, in particular the piezoelectric moduli d_{ijk} and the elastic compliances s_{ijkl} It should be kept in mind, however, that in certain cases it is necessary to introduce factors of 2 (or 4) when changing from the tensor to the matrix notation (see e.g. the book of Nye (N 1)). As an example, for a third-rank tensor:

$$d_{ijk} = d_{in} \text{ when } n = 1, 2 \text{ or } 3, \text{ but}$$

$$2d_{ijk} = d_{in} \text{ when } n = 4, 5 \text{ or } 6.$$

where s^P is the elastic compliance at constant polarization and χ^X is the reciprocal dielectric susceptibility of the crystal under a constant stress. (For $X = 0$, this is the reciprocal susceptibility of the "free" crystal, as distinguished from $\chi^{x=0}$ which is the reciprocal susceptibility of the "clamped" crystal.)

On the other hand, choosing x and E, or X and E as independent variables, respectively, we obtain

$$A(x, E) = \tfrac{1}{2} c^E x^2 + \tfrac{1}{2} k^x E^2 + eEx, \tag{I-3a}$$

and

$$A(X, E) = \tfrac{1}{2} s^E X^2 + \tfrac{1}{2} k^X E^2 - dEX, \tag{I-3b}$$

respectively.

From these free-energy functions, we obtain the following fundamental equations of the piezoelectric crystal. From (I-2a):

$$\left.\begin{aligned} X &= -c^P x + aP, \\ E &= -ax + \chi^x P. \end{aligned}\right\} \tag{I-4a}$$

From (2b):

$$\left.\begin{aligned} x &= -s^P X + bP, \\ E &= bX + \chi^X P. \end{aligned}\right\} \tag{I-4b}$$

From (3a):

$$\left.\begin{aligned} X &= -c^E x + eE, \\ P &= ex + k^x E, \end{aligned}\right\} \tag{I-5a}$$

and from (3b):

$$\left.\begin{aligned} x &= -s^E X + dE, \\ P &= -dX + k^X E. \end{aligned}\right\} \tag{I-5b}$$

The relations between the various coefficients of these equations can be easily obtained by suitable substitutions. For example, if we substitute formally P from (I-5b) into the expression for x in (I-4b), and compare the result with the expression for x in (I-5b) we obtain:

$$\frac{d}{k^X} = b, \qquad s^E - s^P = bd. \tag{I-6}$$

Other useful relations are given in Table III-2.

These relations are particularly interesting in the case where one of the coefficients is found experimentally to exhibit an anomaly at a given temperature. From (I-6), for example, we deduce that if the dielectric susceptibility k^X shows an anomaly (as at the transition temperature of a piezoelectric crystal to a ferroelectric state), either one of the two piezoelectric coefficients d or b should also be anomalous. The experiment shows, as we will see in the following, that it is the piezoelectric modulus d which has an anomaly at the transition temperature. Accordingly, the coefficient b is practically temperature independent, as is the elastic compliance at constant polarization, s^P. Thus, the anomalies of the elastic and piezoelectric behavior can be predicted on the basis of the above thermodynamic treatment.

Let us now make a second step and examine the dielectric behavior of the crystal when it undergoes a ferroelectric transition. To simplify the treatment, we are going to deal only with the free energy as an explicit function of stresses and polarization, $A(X, P)$, and assume that:

(i) all stresses are equal to zero, $X = 0$;

(ii) the polarization vector P is directed along one of the crystallographic axes only; and

(iii) the non-polar phase is centrosymmetrical.

Taking into account the higher-order terms in P, we obtain:

$$A(P) = \tfrac{1}{2}\chi^X P^2 + \tfrac{1}{4}\xi^X P^4 + \tfrac{1}{6}\zeta^X P^6, \tag{I-7}$$

where the coefficients are functions of temperature.

Suppose first that all the coefficients are positive in the non-polar phase. For $P = 0$, $A(0) = 0$, and this value corresponds to a minimum of the free energy.

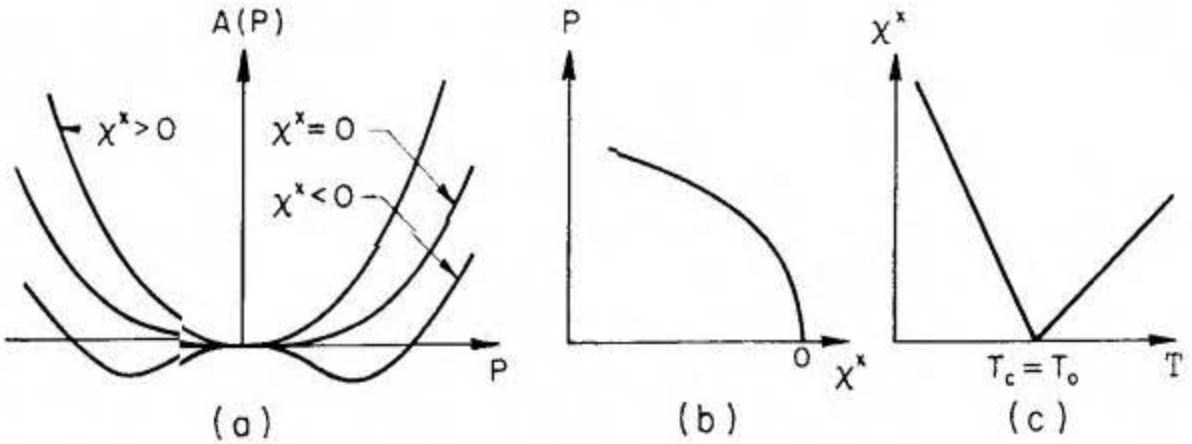

FIG. I-5. Second-order transition (schematic).
(a) Free energy as a function of polarization at temperatures larger than, equal to and lower than the Curie temperature.
(b) Spontaneous polarization as a function of temperature.
(c) Reciprocal susceptibility as a function of temperature.

If we assume at first that only χ^X, the reciprocal free susceptibility, depends on the temperature, while ξ^X and ζ^X are temperature independent, we see that as soon as χ^X becomes negative, the function $A(P)$ will have a maximum for $P = 0$ and two minima for a non-zero value of P. This situation is explained schematically in Fig. I-5(a). The stable state of the crystal will correspond to $P = 0$ for $\chi^X > 0$ and to $P \neq 0$ for $\chi^X < 0$; i.e. the crystal will undergo a ferroelectric transition. The order of the transition is determined, among other things, by the way in which the polarization goes from the value zero to a finite value, i.e. whether the onset of P is continuous or discontinuous. In the present case, P is continuous at the transition: this is a transition of the *second order*. The behavior of P as a function of χ^X, and thus of temperature, is depicted schematically in

Fig. I-5(b). Under these conditions, we can eventually do without the sixth-order term in (I-7) and write for the field E:

$$E = \frac{\partial A}{\partial P} = \chi^X P + \xi^X P^3 \tag{I-8}$$

whence, putting $E = 0$ (*spontaneous* polarization):

$$P^2 = -\frac{\chi^X}{\xi^X}. \tag{I-9}$$

It follows that the reciprocal suspectibility is, *above* the transition:

$$\left(\frac{\partial^2 A}{\partial P^2}\right)_{P=0} = \chi^X,$$

below the transition:

$$\left(\frac{\partial^2 A}{\partial P^2}\right) = \chi^X + 3\,\xi^X P^2$$

i.e. using (I-9),

$$\left(\frac{\partial^2 A}{\partial P^2}\right) = -2\,\chi^X. \tag{I-10}$$

The temperature dependence of χ^X is depicted schematically in Fig. I-5(c); the dielectric susceptibility of the free crystal becomes infinite at the transition temperature.

Equation (I-8) gives us information about the P–E relationship below the transition temperature T_c. Owing to the fact that χ^X becomes negative below T_c, the P–E curve has the character shown in Fig. I-6 by the curve $ABCD$. The portion BC

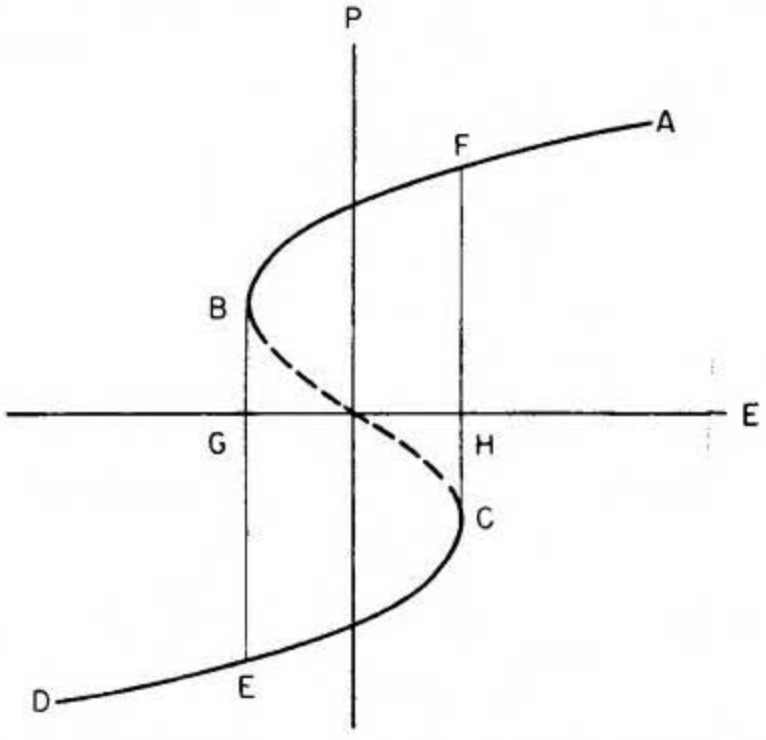

Fig. I-6. Second-order transition: polarization as a function of field below the Curie point.

of the curve corresponds to an unstable state; the crystal jumps directly from the state B to E and from C to F. A coercive field E_c is thus predicted with the magnitude given by $GH/2$. The theoretical value of the coercive field, however, always turns out to be one or two orders of magnitude larger than the observed value. This is because the present theoretical treatment assumes that the reversal of the polarization of the whole crystal takes place in one single step. In reality, the reversal mechanism consists of nucleation and growth of new domains (see, e.g. Section II-7), processes which proceed by steps and require time. Thus, the experimental coercive field E_c is not only dependent on the amplitude but also on the frequency of the applied a.c. field.

Abandoning now the assumption that all coefficients in (I-7) are positive above the transition, we assume, for example, that ξ^X is negative and ζ^X is positive. This means that it is possible for the free-energy function to have two equal minima, one for $P = 0$ and the other for $P \neq 0$, at the same value of $\chi^X > 0$, i.e. at the same temperature. The stable state of the crystal will jump from one with $P = 0$ to one with $P = P_0$ *discontinuously* at this (transition) temperature: this transition is of the *first order* (Fig. I-7).*

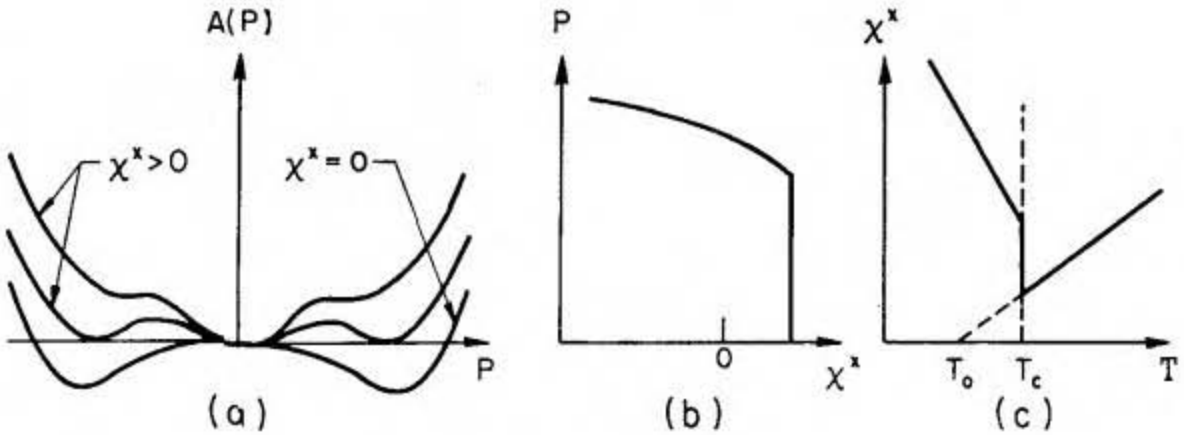

FIG. I-7. First-order transition (schematic).
(a) Free energy as a function of polarization at temperatures larger than, equal to and lower than the Curie temperature.
(b) Spontaneous polarization as a function of temperature.
(c) Reciprocal susceptibility as a function of temperature.

We compute the values of $P = P_0$ and $\chi^X = \chi_0^X$ at the transition by considering that the values of the free energy for $P = 0$ and $P = P_0$ must be equal at this temperature:

$$A(0) = \tfrac{1}{2}\chi^X P^2 + \tfrac{1}{4}\xi^X P^4 + \tfrac{1}{6}\zeta^X P^6 = 0. \qquad \text{(I-11)}$$

* Experimentally, it is often difficult to establish whether or not the polarization (or other quantities such as volume, entropy, etc.) is discontinuous at the transition temperature. For this reason, it has been suggested that a better definition of a first order transition is coexistence of the two phases in equilibrium at the transition temperature, so that a definite phase boundary is formed (see, e.g. Smoluchowski (S 4)). This definition, however, is also subject to experimental limitations.

On the other hand, the field E must be zero for the polarization to be spontaneous:

$$\frac{\partial A}{\partial P} = E = \chi^X P + \xi^X P^3 + \zeta^X P^5 = 0. \tag{I-12}$$

From (I-11) and (I-12) we obtain:

$$P_0^2 = \frac{3}{4}\left(-\frac{\xi^X}{\zeta^X}\right), \tag{I-13}$$

$$\chi_0^X = \frac{3}{16}\left(\frac{\xi^X}{\zeta^X}\right)^2, \tag{I-14}$$

showing that a discontinuous change in P occurs at the transition (Fig. I-7b) and the value of χ^X at the transition, χ_0^X, is positive. The temperature dependence of χ^X is shown schematically in Fig. I-7(c): the dielectric suspectibility of the free crystal is finite but discontinuous at the transition temperature.

The simple thermodynamic treatment reported above is thus able to describe the essential features of a ferroelectric transition of the first or second order by assuming that only χ^X, the reciprocal dielectric susceptibility, is a function of the temperature. Actually, this is not strictly correct, as the other coefficients of the free-energy expansion could also be temperature dependent, but this fact does not much change the overall picture. We are going to see in the following chapters that the above thermodynamic theory can be extended to predict, for example, the heat of transition, the effect of mechanical stresses or electric fields on the transition, the optical anomalies, etc. Also, the treatment will be extended to those types of transition which involve a change in direction of polarization, as in the ferroelectrics of the perovskite class.

Two further remarks are necessary to this introductory treatment of the thermodynamics of crystals. The first is that the phenomenological theory of ferroelectrics outlined above by its nature is only an approximation. This is so not only because we make use of a finite number of terms of the free-energy expansion, but also because we assume that the same function can be used both for the non-polar and the polar phase. The latter assumption can be justified, at this stage, by the fact that the polar phases are obtained through very slight distortions of the non-polar phases.

The second remark is concerned with the implication contained in the above treatment, that the ferroelectric phenomenon has a dielectric origin. Thus, the coefficient of P^2 in the free-energy expansion bears the significant temperature dependence, and the anomalies of the piezoelectric, elastic and other properties are thought to be a mere consequence of the anomalous dielectric behavior. This is certainly true for a number of ferroelectric crystals, such as Rochelle salt, potassium di-hydrogen phosphate, barium titanate and tri-glycine sulfate, but, as pointed out in Section 1, may be incorrect for other, less spectacular, ferroelectrics.

The thermodynamic treatment outlined above will be extended and applied to specific cases in the following chapters, in particular, to the most typical ferroelectrics just mentioned. For a quick survey of where, in this book, the thermodynamic and other theories are discussed, the reader is referred to Appendix II.

6. Antiferroelectricity

In considering the alignment of electric dipoles within a ferroelectric crystal, we must keep in mind that this co-operative phenomenon is governed by two essentially different types of interaction forces. Forces due to chemical bonds, van der Waals attraction, repulsion forces and others have all such short ranges that, usually, interaction between nearest neighbors only need be considered. In contrast to these forces, those due to dipolar interaction have a very long range. Consequently, an accurate calculation of the interaction between a particular dipole and all the other dipoles of a given sample is generally quite complicated.

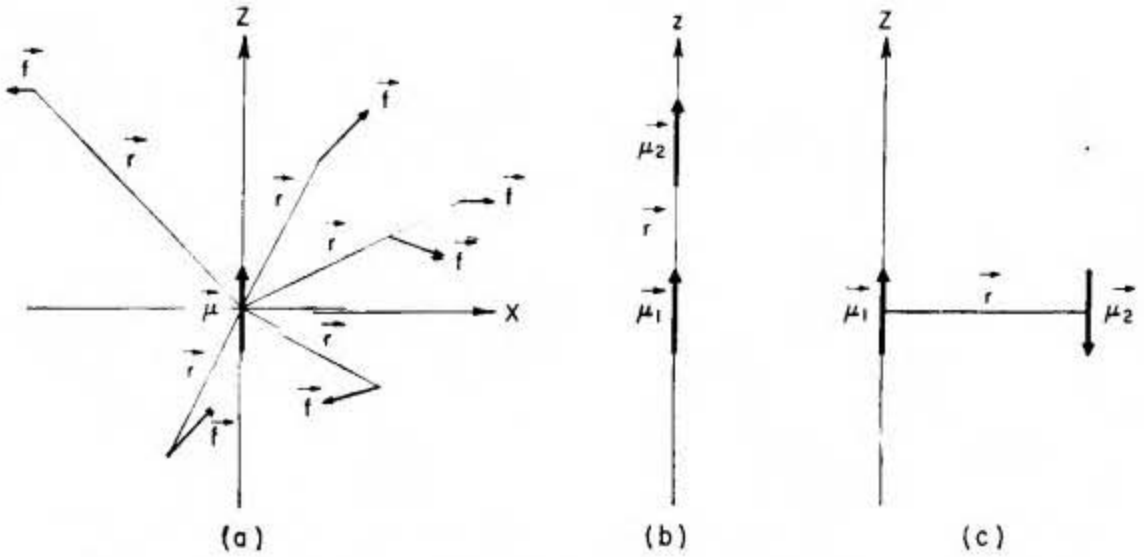

FIG. I-8. (a) The intensity of the dipole field $\boldsymbol{f}$ (according to Böttcher (B 1)). (b) Parallel dipoles (see text). (c) Antiparallel dipoles (see text).

It may be useful to recall the characteristics of the dipole field. Given a point dipole at the origin of a rectangular co-ordinate system x, y, z, the field strength $\boldsymbol{f}$ caused by this dipole at a point located at the distance $\boldsymbol{r}$ from the origin is given by the formula

$$\boldsymbol{f} = \frac{3\boldsymbol{\mu}_1 \cdot \boldsymbol{r}}{r^5} \cdot \boldsymbol{r} - \frac{\boldsymbol{\mu}_1}{r^3}, \tag{I-15}$$

where $\boldsymbol{\mu}_1$ is the dipole moment. If the z-axis is along the dipole vector, the relative values of $\boldsymbol{f}$ at some points in the xz plane are shown in Fig. I-8(a). If we now bring another point dipole $\boldsymbol{\mu}_2$ at the point with co-ordinates $\boldsymbol{r}(x, y, z)$, the interaction energy between the two dipoles $\boldsymbol{\mu}_1$ and $\boldsymbol{\mu}_2$ is given by the work required to bring the second dipole from infinity at the location $\boldsymbol{r}$ (see, e.g., Böttcher (B 1)):

$$W = -\boldsymbol{f} \cdot \boldsymbol{\mu}_2 = -\frac{3}{r^5}(\boldsymbol{\mu}_1 \cdot \boldsymbol{r})(\boldsymbol{\mu}_2 \cdot \boldsymbol{r}) + \frac{\boldsymbol{\mu}_1 \boldsymbol{\mu}_2}{r^3}. \tag{I-16}$$

It is easily seen that the minimum value of the interaction energy W is obtained when $\boldsymbol{\mu}_1$, $\boldsymbol{\mu}_2$ and $\boldsymbol{r}$ all have the same direction (Fig. I-8b), in which case:

$$W = -\frac{2\boldsymbol{\mu}_1 \boldsymbol{\mu}_2}{r^3}. \tag{I-17}$$

The maximum value of W is reached when one of the dipoles has the same direction as $\boldsymbol{r}$ and the other the opposite direction:

$$W = \frac{2\mu_1\mu_2}{r^3}.$$

When both dipoles are perpendicular to $\boldsymbol{r}$ and antiparallel to each other (Fig. I-8c), the interaction energy is

$$W = -\frac{\mu_1\mu_2}{r^3}, \tag{I-18}$$

but if they are parallel to one another, $W = \mu_1\mu_2/r^3$.

Thus, it is seen that when both dipoles are parallel to $\boldsymbol{r}$, then the parallel arrangement is stable; when both are perpendicular to $\boldsymbol{r}$, then the antiparallel arrangement is more stable. This is true, of course, only for two isolated point dipoles.

If we next bring a large number of point dipoles (which, for simplicity, we will assume to be all equal) at the lattice points of a given lattice, then the total

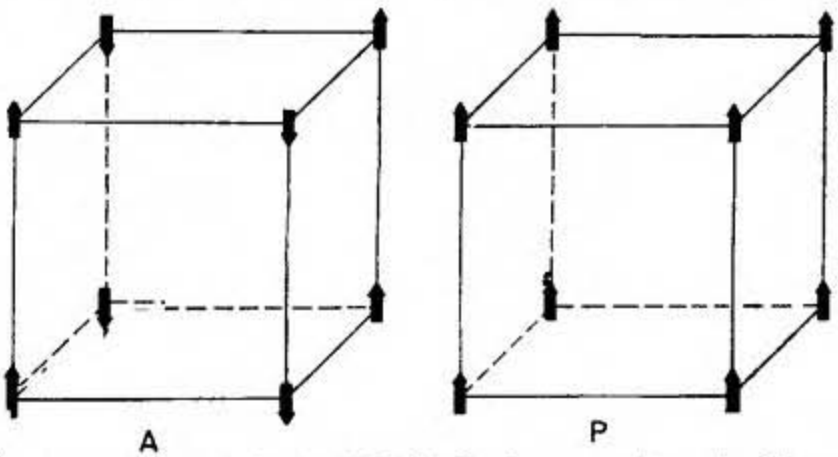

FIG. I-9. Antiparallel (A) and parallel (P) dipole arrays in a simple cubic lattice.

dipolar interaction energy of the crystal thus obtained will obviously be a function of the orientations chosen for each dipole. If we allow either parallel or antiparallel orientation only, we are theoretically in the position to compute whether, for the given lattice, the arrangement of all dipoles parallel to each other corresponds to a lower value of the interaction energy than any other arrangement, involving antiparallel dipole orientations. These calculations are obviously quite complicated, but in a few simple cases they can be performed. In the case of a simple cubic lattice, for example, Luttinger and Tisza (L 1) were able to show that the antiparallel dipole array indicated with the letter A in Fig. I-9 has the lowest energy of all possible arrays in this lattice, including that involving parallel orientation of the dipoles (P in Fig. I-9).

The unit cell of the antiparallel dipole lattice A, however, is no longer primitive. The periodicity of this lattice must be multiplied by two in the directions perpendicular to the dipole axis. The lattice can be looked upon as being built by two interpenetrating sublattices, each of which is occupied by dipoles orientated parallel to each other, but the polarities of the two sublattices are antiparallel to each other. Just as we call *polar* the crystal which has the lattice denoted by

the letter P in Fig. I-9, we are going to call *antipolar* the crystal characterized by the lattice A in the same figure. Thus we call antipolar the crystals which are characterized by the existence of two oppositely polarized sublattices.

Antiparallel dipole arrangements actually do occur, in lattices which are more complicated than the simple cubic. Moreover, it is possible to encounter substances which, at a certain temperature, undergo a transition from a non-polar to an antipolar state. Dielectrically, such a transition may or may not be detectable, but calorimetric measurements and, above all, accurate structural analyses ought to be able to detect this type of transition. A typical example of the case in which a transition from a non-polar into an antipolar phase can be detected by dielectric measurements is that of ammonium di-hydrogen phosphate, $NH_4H_2PO_4$, isomorphous with KH_2PO_4, whose dielectric constant drops anomalously, upon cooling, at the transition temperature of about -126 °C.

It should be noticed that, according to the definition, an antipolar crystal should always have a superlattice below the transition from a non-polar phase. However, it is not always necessary for such a superlattice to be characterized by a multiple unit cell, as was the case, above, for a simple cubic lattice. If the unit cell of the non-polar phase happens to contain an even number of equivalent molecular groups, a multiple unit cell may not be necessary in the antipolar state.

So far, our definition of an antipolar crystal was given according to a logical parallelism with that of a polar crystal. The latter case occurs, obviously, when the energy corresponding to a parallel dipole orientation is a minimum. We know that, in most such cases, the dipole interaction is such as to give a rigid dipole array, i.e. a pyroelectric crystal. From the dielectric point of view, however, such cases are not very interesting. They become interesting only when the contributions to the interaction energy are so delicately balanced as to give a rather loosely bound array of parallel dipoles. In this case, the direction of the spontaneous polarization can be reversed with an external field and we have a ferroelectric crystal. In the thermodynamic language, we may say that, in a ferroelectric crystal, the free energy of the polar state is comparable to the free energy of the non-polar state.

Similarly, in an antipolar crystal the dipole interaction may be such as to give a rigid array of antiparallel dipoles. Again, such a case is rarely interesting from the dielectric point of view. It becomes interesting only if the coupling between the dipoles is such that the interaction energy is comparable to that of a polar crystal. In terms of thermodynamics, we may say that the free energy of the antipolar state is comparable to that of the polar state. When this is the case, then we say that the crystal considered is *antiferroelectric*. Accordingly, we define an antiferroelectric crystal as an antipolar crystal whose free energy is comparable to that of a polar crystal. This definition is in line with that of a ferroelectric crystal. Just as x-ray methods, for example, may be able to establish the polarity of a given crystal, but only dielectric methods can establish its ferroelectric activity, so can the antipolar character of a crystal be established, eventually, by x-ray methods, but only dielectric measurements can definitely establish its antiferroelectric character.

How can this be done? There are two consequences of our definition of an antiferroelectric crystal which affect its dielectric behavior. In the first place, when a crystal undergoes a transition from a completely unpolarized to such an antiferroelectric state, it will show a pronounced dielectric anomaly at the antiferroelectric transition point. This large anomaly is not directly associated with the antipolar phase, but is a consequence of the existence of a ferroelectric state with comparable free energy. In this case, we are experimentally able to observe the dielectric anomaly at the transition, but we will not observe dielectric hysteresis in the low-temperature phase. It is actually *because* of the observability of these particular antiferroelectric transitions that the concept of antipolarity and antiferroelectricity has become important in the physics of dielectric materials and is usually closely associated to the phenomenon of ferroelectricity.

The second consequence of only a small difference between the free energies of ferro- and antiferro-electric states is that it is possible, in antipolar phases of this kind, to decrease the free energy of the polarized state more than that of the antipolarized state by means of external mechanical or electrical stresses. At sufficiently high field strengths, antiferroelectric crystals become ferroelectric, although not necessarily along the same axis. Generally, the application of large electric fields induces a phase transition; the crystal lattice undergoes a rearrangement and the polar axis of the induced phase is not directed along the former antipolar direction. In antiferroelectric, *orthorhombic* $PbZrO_3$, for example, application of strong electric fields can induce a ferroelectric *rhombohedral* phase.

It should be emphasized, at this point, that the mere fact that a crystal exhibits a dielectric anomaly but no dielectric hysteresis on either side of the transition temperature is not sufficient to label the crystal as antipolar or antiferroelectric. Generally, a detailed structure analysis is required to establish whether the atomic shifts along a certain crystallographic direction are antiparallel. Alone, this analysis is again not sufficient to prove the existence of an antiparallel "polarization" but this does not invalidate the fact that the phenomenological behavior of the crystal can be understood in terms of sublattices with opposite polarizations.

From the above description it should be clear that the phenomena of ferroelectricity and antiferroelectricity are related to a given crystallographic *direction* within a crystal. In other words, a crystallographic direction may be polar, antipolar or non-polar. Thus, it is not difficult to conceive spatial arrays which may cause a crystallographic direction to be polar and another, perpendicular to it, antipolar. In this case, the corresponding crystal may exhibit ferroelectric properties along the one axis and antiferroelectric properties along the other axis. A new name has been introduced for such crystals, namely *ferrielectric*, but what we have said above should make this increase in nomenclature unnecessary.

With the exception of a few special cases, this book is not going to be concerned further with the description and the theories of antiferroelectric crystals. Only the cases of the perovskite antiferroelectric crystals lead zirconate, $PbZrO_3$, and sodium niobate, $NaNbO_3$ are going to be discussed (see Chapter V). The general problem of antiferroelectricity has been treated by Kittel (K 3) and Takagi (T 1) and reviewed by Känzig (K 1) and Forsbergh (F 1).

BIBLIOGRAPHY

(B 1) Böttcher, C. J. F., *Theory of Electric Polarization*, Elsevier, Amsterdam (1952).

(B 2) Brown, W. F., *Dielectrics, Handbuch der Physik*, Vol. 17, pp. 1–154, Springer-Verlag, Berlin (1956).

(C 1) Cady, W. G., *Piezoelectricity*, McGraw-Hill, New York (1946).

(D 1) Dekker, A. J., *Solid State Physics*, Prentice-Hall, Englewood Cliffs, N. J. (1958).

(D 2) Devonshire, A. F., Theory of ferroelectrics, *Phil. Mag.* Suppl. 3, 85 (1954).

(F 1) Forsbergh, P. W., Jr., *Piezoelectricity, Electrostriction and Ferroelectricity, Handbuch der Physik*, Vol. 17, pp. 264–392, Springer-Verlag, Berlin (1956).

(F 2) Fröhlich, H., *Theory of Dielectrics*, Clarendon Press, Oxford (1949).

(J 1) Jaynes, E. T., *Ferroelectricity*, Princeton University Press, Princeton (1953).

(K 1) Känzig, W., *Ferroelectrics and Antiferroelectrics, Solid State Physics*, Vol. 4, pp. 1–197, Academic Press, New York (1957).

(K 2) Kittel, C., *Introduction to Solid State Physics*, John Wiley, New York (1956).

(K 3) Kittel, C., *Phys. Rev.* **82**, 729 (1951).

(L 1) Luttinger, J. M. and Tisza, L., *Phys. Rev.* **70**, 954 (1946).

(M 1) Megaw, H. D., *Ferroelectricity in Crystals*, Methuen, London (1957).

(M 2) Mueller, H., *Ann. N. Y. Acad. Sci.* **40**, 321 (1940).

(N 1) Nye, J. F., *Physical Properties of Crystals*, Clarendon Press. Oxford (1957).

(S 1) Sawyer, C. B. and Tower, C. H., *Phys. Rev.* **35**, 269 (1930).

(S 2) Smyth, C. H., *Dielectric Behavior and Structure*, McGraw-Hill, New York (1955).

(S 3) Smith, C. S., *Macroscopic Symmetry and Properties of Crystals, Solid State Phyiscs*, Vol. 6, pp. 175–249, Academic Press, New York (1958).

(S 4) Smoluchowski, R., *Phase Transformations in Solids, Handbook of Physics*, pp. 8–110, McGraw-Hill, New York (1958).

(T 1) Takagi, Y., *Phys. Rev.* **85**, 315 (1952).

CHAPTER II

TRI-GLYCINE SULFATE AND ISOMORPHOUS CRYSTALS

1. Introduction

Tri-glycine sulfate is a relatively young member of the fast-growing family of ferroelectric crystals. It has immediately attracted the attention of many researchers because it exhibits ferroelectric properties at room temperature, and it can be grown easily in large samples. Chemically and crystallographically, it is by far not the simplest ferroelectric known, but its phenomenological behavior is very simple. It represents, in fact, one of the most typical examples of a ferroelectric whose behavior fits quite perfectly the description that we have given in Chapter I. This is the reason why we treat it first.

The ferroelectric activity of tri-glycine sulfate, $(NH_2CH_2COOH)_3 \cdot H_2SO_4$, (abbreviated TGS), was discovered by Matthias *et al.* (M 1) in 1956. The Curie temperature lies at 49 °C. The phase above the transition has monoclinic symmetry and belongs to the centrosymmetrical class $2/m$. Below the transition temperature, the mirror plane disappears and the crystal belongs to the polar point group 2 of the monoclinic system. Ferroelectricity is found along the direction of the twofold polar axis (monoclinic b axis). The transition is of the second order.

Ferroelectricity occurs also in two crystals isomorphous with TGS. They are: tri-glycine selenate, $(CH_2NH_2COOH)_3 \cdot H_2SeO_4$, (abbreviated TGSe), with transition temperature 22 °C (M 1), and tri-glycine fluoberyllate, $(CH_2NH_2COOH)_3 \cdot H_2BeF_4$ (abbreviated TGFB), with Curie temperature 70 °C (P 1). The characteristics of these transitions are similar to those found in TGS.

Large crystals of these compounds can be grown easily from water solutions prepared by reacting an aqueous glycine solution with the proper amount of the corresponding (sulfuric, selenic or fluoberyllic) acid. The growth can be achieved by slow evaporation of the solvent at constant temperature or by slowly lowering the temperature at constant supersaturation. A more sophisticated method has been described by Nitsche (N 1), who reported also the temperature dependence of the solubility curves.

The habit of the crystals obtained depends somewhat on the growing procedure and is generally quite complex owing to the presence of many faces. The b faces, perpendicular to the monoclinic b axis, are mostly absent or very small, but the crystals have a pronounced cleavage plane parallel to (010). Thus, crystal plates oriented perpendicularly to the polar axis can be easily obtained by cleavage of larger crystals with no need of knowing the directions of the monoclinic a and c axes.

However, the investigation of the dielectric, piezoelectric and elastic tensors requires the choice and the identification of a reference system of co-ordinates. Since the most convenient monoclinic angle β is approximately equal to 105° and the predominant face is often the c face, the following orientation of a reference systems of orthogonal co-ordinates is selected in relation to the most common crystal habit (K 1). The Y axis is parallel to the polar axis, the Z axis is parallel to the natural edge which forms an angle 105° with the predominant (c) face of the crystal, and the X axis is perpendicular to Y and Z to form a right-handed system, as indicated in Fig. II-1.

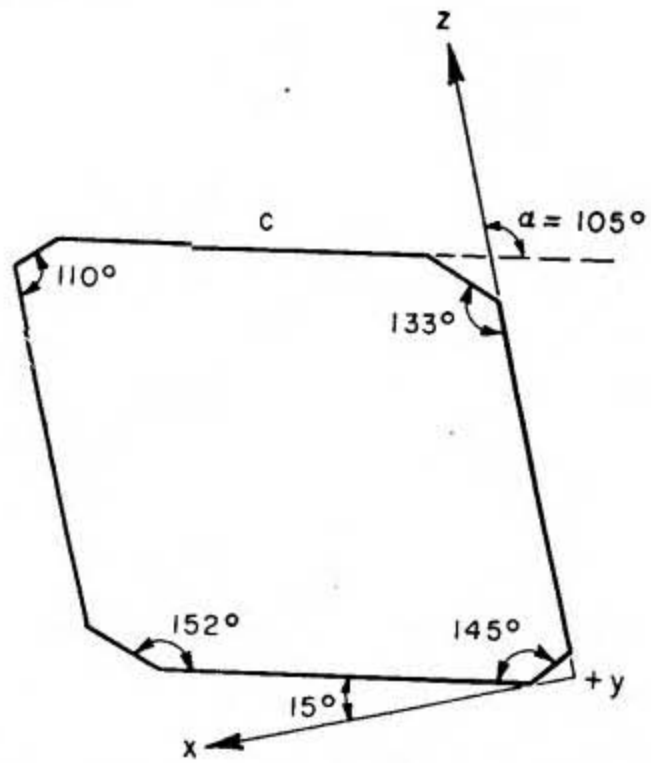

FIG. II-1. Reference system of co-ordinates in a crystal of tri-glycine sulfate (according to Konstantinova *et al.* (K 1)).

2. Dielectric Properties

The components of the dielectric constant tensor of TGS have the following values at 23 °C (measuring field 1 V/cm, frequency 500 kc/s) (K 1):

$$\varepsilon_a = 8.6, \quad \varepsilon_b = 43, \quad \varepsilon_c = 5.7^*$$

The temperature dependence of these quantities, measured at 1 kc/s and 1 V/cm is shown graphically in Fig. II-2 (H 1). The component $\varepsilon_{22} = \varepsilon_b$, measured along the polar axis, is the most important quantity and will therefore be referred to, in the following, as the dielectric constant ε. It shows a very pronounced anomaly in the vicinity of the transition temperature T_c. The actual peak value is determined by unavoidable inhomogeneities of temperature and stress distri-

* It should be noted that ε_c is not the dielectric constant measured perpendicularly to the c face but that measured along the Z axis of Fig. II-1.

butions, and also by the quality of the electrodes, as these may cause partial clamping of the crystal. Peak values of ε greater than 10^5 have been measured (T 1).

The constants $\varepsilon_{11} = \varepsilon_a$ and $\varepsilon_{33} = \varepsilon_c$ are practically independent of temperature.

The dielectric constant ε follows the Curie–Weiss law $\varepsilon \cong C/(T - T_0)$ in the vicinity of the transition temperature, as shown by the plot of $1/\varepsilon$ vs. temperature (T 1) (Fig. II-3). The Curie constant C is equal to 3200 °K, but variations of

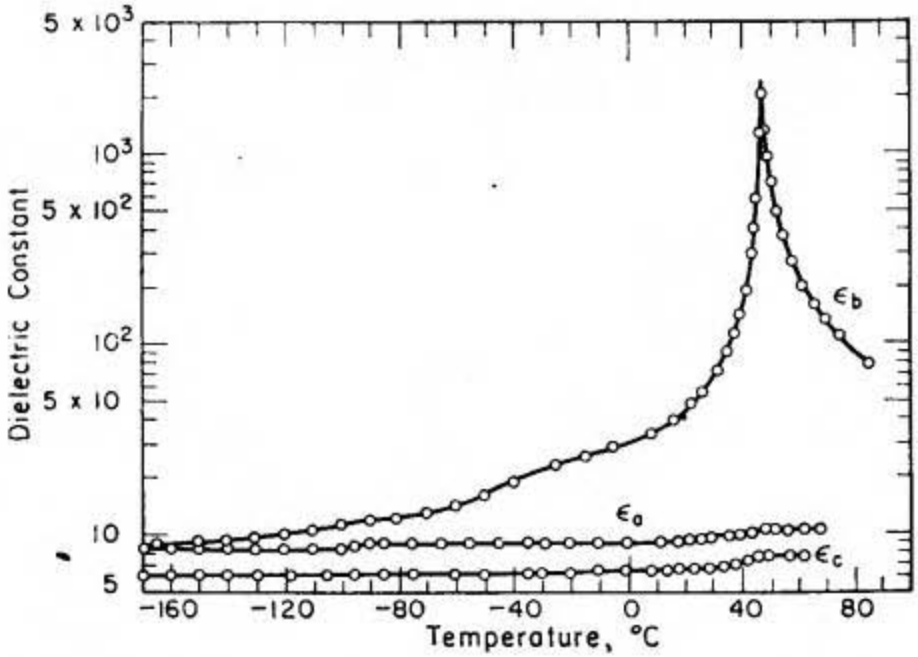

FIG. II-2. Dielectric constant of tri-glycine sulfate as a function of temperature (according to Hoshino *et al.* (H 1)).

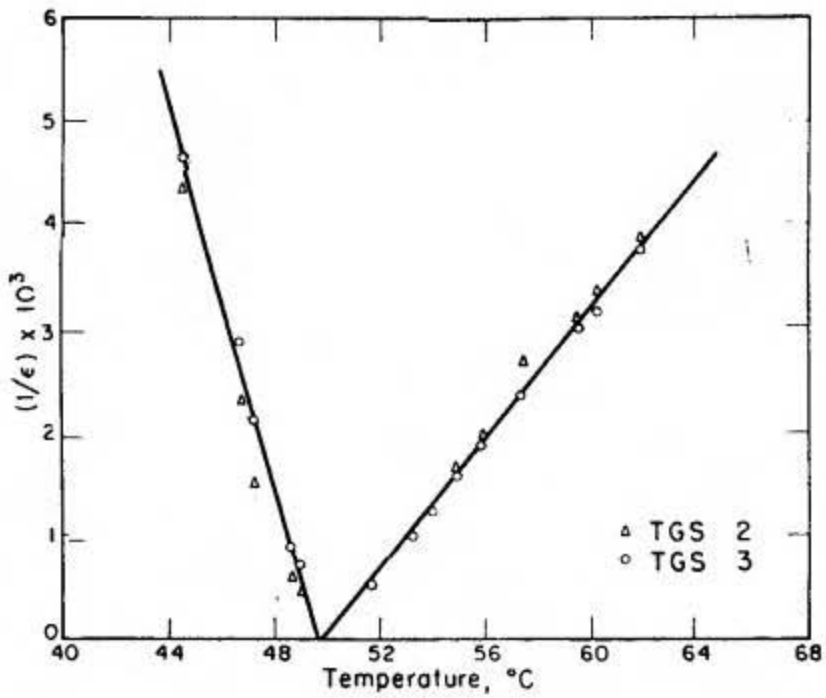

FIG. II-3. Curie–Weiss law for tri-glycine sulfate (according to Triebwasser (T 1)).

about 10% can be found in different specimens (H 1). The Curie–Weiss temperature T_0 agrees practically with the Curie temperature $T_c = 49$ °C. High-frequency measurements of the dielectric constant were carried out by Nishioka and Takeuchi (N 2). At 9600 Mc/s, the room-temperature values of the dielectric constant and the loss factor were reported to be $\varepsilon = 20$ and $\tan \delta = 0.043$, respectively, indicating that dielectric relaxation is already effective in the microwave region. The dielectric anomaly at the Curie temperature is, however, still present at the frequency employed (see also Lurio and Stern (L 1) and Nakamura and Furuichi (N 3)).

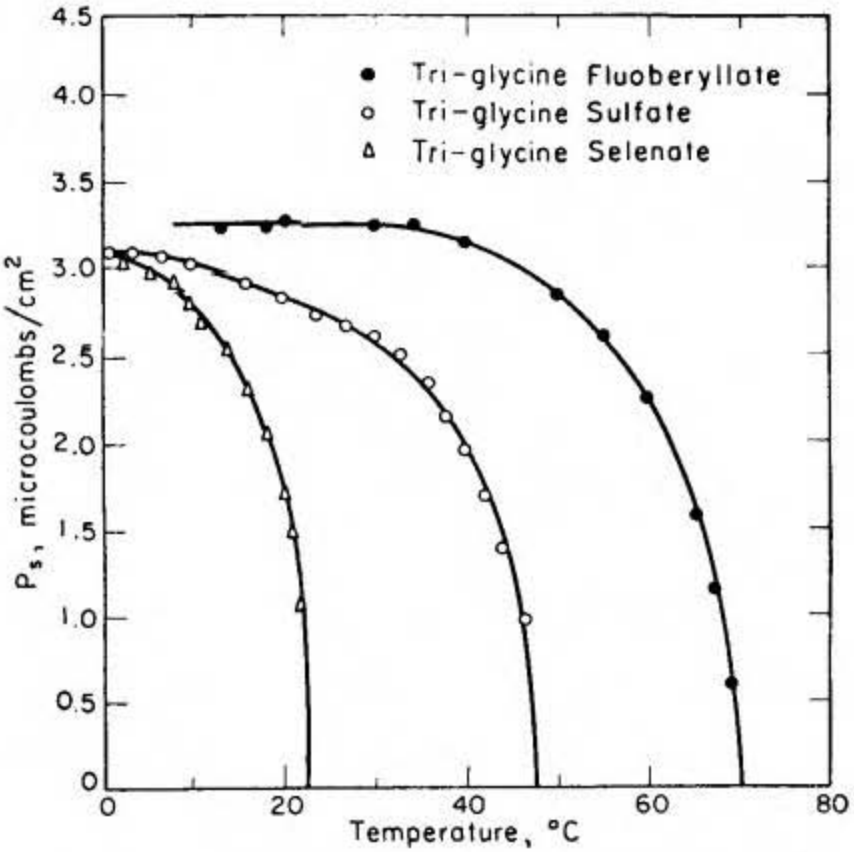

FIG. II-4. Spontaneous polarization P_s of tri-glycine sulfate (H 1), tri-glycine fluoberyllate (H 1) and tri-glycine selenate as a function of temperature.

The temperature dependence of the spontaneous polarization P_s is depicted in Fig. II-4, and is typical of a transition of the second order. The value of P_s at room temperature is about 2.8×10^{-6} C/cm^2 (H 1), but the data reported by different authors may fluctuate within $\pm 20\%$ of this value (T 2), (T 3), (D 1), (Z 1). Below 0 °C, the spontaneous polarization increases only slowly with decreasing temperature, reaching a value of approximately 4.3×10^{-6} C/cm^2 at -140 °C (C 4).

The pyroelectric effect was investigated at room temperature by Savage and Miller (S 2), and down to -140 °C by Chynoweth (C 4), with the dynamic technique first introduced by Chynoweth and described in Section IV-2. The pyroelectric hysteresis loops may sometimes appear to be biased in the direction of the polarization axis, when precautions are not taken to eliminate electrode-

edge effects. The technique allowed Chynoweth to establish that the polarization can still be reversed at temperatures as low as -140 °C, but reversal may take several seconds for applied fields of the order of 10^3 V/cm. Above the Curie point, where the structure of TGS is centrosymmetric, no pyroelectric effect should be expected, but Chynoweth (C 4) has found that small pyroelectric signals can be generated, temporarily, at temperatures appreciably higher than T_c. Upon heating a previously polarized crystal, the pyroelectric signal first passes through a sharp peak at the Curie point, then drops rapidly to zero but finally builds up again in the opposite direction. As the temperature continues to rise, this residual signal passes through a maximum and then decays to zero in a few minutes. If the temperature is then lowered, the pyroelectric signal does not reappear until the Curie point is approached. The cause of the residual signal has thus been "annealed out". It has also been found that the sign of the residual signal cannot be affected by applying polarizing fields with opposite direction at room temperature. These unexpected effects have been explained by Chynoweth in terms of compensation charges accumulated around residual domains. It has namely been established that a number of narrow domains may persist in a crystal at room temperature even when strong d.c. fields are applied (see Section 7). Free compensation charges are expected to accumulate on the domain boundaries of these residual domains, and when the spontaneous polarization vanishes, as it does when the crystal is heated through the Curie point, these charges are left behind and take some time to disappear. While they last, they *induce* a polarization that is the cause of the residual pyroelectric signals. It was found that fields of the order of 10^2–10^3 V/cm had to be applied to the crystal above the Curie point to induce a pyroelectric signal comparable to the residual signal. The annealing out of the residual signal would thus be ascribed to the gradual annihilation of the compensation charges around the old domain locations.

It has also been established that a TGS crystal cooled through the Curie temperature shows a marked tendency to repolarize in the same direction in which it was previously poled. This effect has been assumed to be due to the existence of a thin layer with no (or zero net) polarization at the surface of the crystal. Bearing no spontaneous polarization, such a surface layer would not take part in the process of polarization reversal, and hence would give rise to compensation charges at the interface between bulk and surface layer. The field produced by these interface charges, while they last, throughout the bulk of the crystal may be small but quite sufficient to cause the whole crystal to repolarize in the same sense as it cools through the Curie point, since the coercive field vanishes at the Curie point. The nature of the postulated surface layer is not well understood, at present, but may tentatively be conceived of as a chemical disturbance or a mechanical distortion of the crystal structure at the surface. The thickness of this layer was tentatively estimated to be within 10^{-7} cm and 10^{-5} cm (C 4).

Measurements of the coercive field E_c of TGS have been carried out by a number of authors (T 3), (D 1), (T 2). As was pointed out in Section I-5, this quantity is strongly dependent upon the amplitude and frequency of the applied

field, at any given temperature below the Curie point. At room temperature, the value of E_c measured with a field of 1500 V/cm and a frequency of 50 c/s is equal to 430 V/cm (D 1). The dependence of the 50 c/s coercive field upon the amplitude of the applied field has been tentatively written by Toyoda *et al.* (T 3) in the form

$$E_c = \text{constant} \times E_{max}^{b},$$

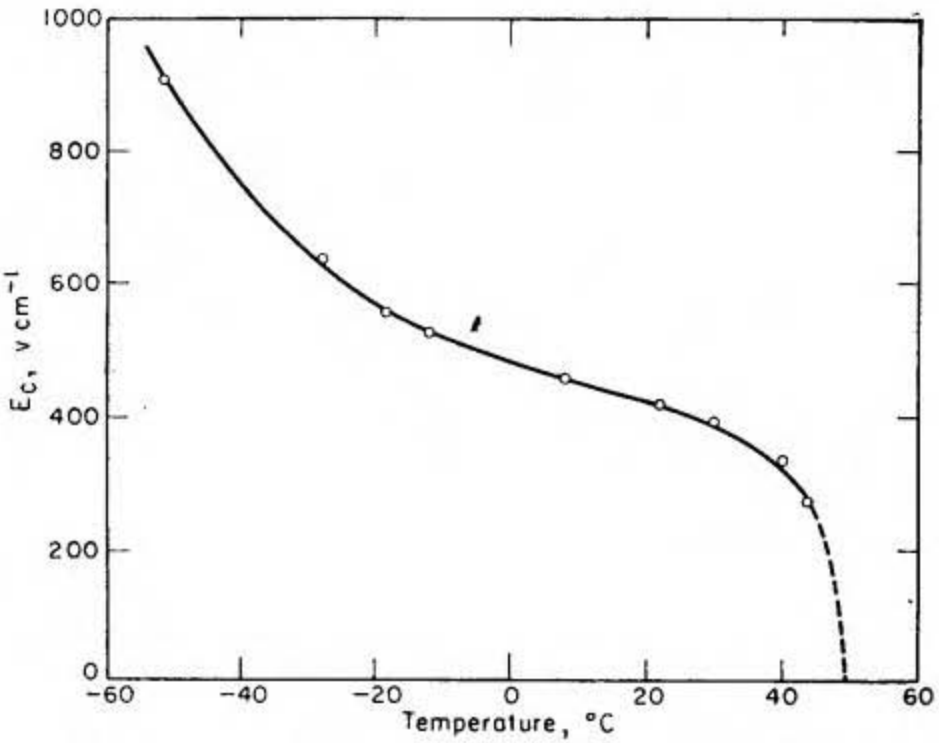

FIG. II-5. Coercive field E_c of tri-glycine sulfate, measured with a field of 1500 V/cm at 50 c/s as a function of temperature (according to Domanski (D 1)).

where the exponent b equals 0.5 at 20 °C and 0.4 at -73 °C. The temperature dependence of E_c measured with a 50 c/s field of 1500 V/cm is depicted in Fig. II-5. The sharp increase occurring below -10 °C is not indicative of phase transitions, but of the fact that the relaxation time associated with the reversal process increases rapidly with decreasing temperature.

3. Thermodynamic Theory and Dielectric Non-linearity

As we mentioned in Section 1, the phenomenological theory of TGS is very simple. Qualitatively, it is already contained in the general thermodynamic treatment outlined in Section I-5. We will presently consider the quantitative aspects of this treatment and we will see, on the basis of the agreement between theory and experiment, that the essential features of a ferroelectric transition such as that of TGS can be described satisfactorily on the basis of the expansion of the free-energy function *in terms of polarization only.*

The experimental results described in the preceding section are strongly indicative of the fact that the ferroelectric transition in TGS is of the second order. We refer, in particular, to the fact that the spontaneous polarization P_s

is a continuous function of temperature and the dielectric constant becomes extremely large at the Curie temperature. In addition, thermal expansion measurements have revealed no abrupt change in volume at the Curie point (E 2).

Since we are only interested in the dielectric behavior along the monoclinic b axis, we are going to consider the polarization and field components in this direction only, i.e. we put

$$P_1 = P_3 = 0, \quad E_1 = E_3 = 0 \quad \text{and} \quad P_2 = P, \quad E_2 = E.$$

We then can write the free energy of the stress-free crystal in the non-polar phase (Eq. I-7) as follows:

$$A(P, T) = \frac{2\pi}{C}(T - T_0)P^2 + \tfrac{1}{4}\xi P^4 + \tfrac{1}{6}\xi P^6. \tag{II-1}$$

The coefficient of P^2 is written in such a way as to take care of the experimentally proven existence of the Curie–Weiss law. The superscript X of the coefficients ξ^X and ζ^X (Eq. I-7), indicating that these quantities are measured at constant (zero) stress, is dropped for convenience. Moreover, we assume, in the first approximation, that the coefficients ξ and ζ are independent of temperature, at least in the vicinity of the transition.

Under these assumptions, we can derive the temperature dependence of the spontaneous polarization P_s from (II-1) and see how it fits the experimental data, as indicated by Triebwasser (T 1). The partial derivative $(\partial A/\partial P)_T = E$ gives us an equation for P_s when we put $E = 0$. A simple solution of this equation can be written if we assume that we are sufficiently close to the transition temperature for the polarization to be small. We obtain (T 1):

$$P_s^2 = \frac{4\pi}{\xi C}(T_0 - T) - \frac{16\pi^2}{C^2}\frac{\zeta}{\xi}(T_0 - T)^2. \tag{II-2}$$

By the least square fitting of the experimental P_s^2 vs. $(T_0 - T)$ curve in the vicinity of the transition temperature, the coefficients ξ and ζ can be determined. The results are (T 1):

$$\xi = 8.0 \times 10^{-10}\ (\text{e.s.u./cm}^2)^{-2}; \quad \zeta = 5.04 \times 10^{-18}\ (\text{e.s.u./cm}^2)^{-4}.$$

We are now in the position to check quantitatively how well the power series expansion (II-1) converges in the temperature range of interest to us. Evaluating the terms in P^2, P^4 and P^6 at about 40 °C, where $P \cong 2 \times 10^{-6}$ C/cm^2, we find that they contribute 7.3×10^5 ergs/cm^3, 2.6×10^5 ergs/cm^3, and 0.4×10^5 ergs/cm^3, respectively. Thus, we are justified in dropping the term in P^6 from expression (II-1), for convenience. In this approximation, Eq. (II-2) predicts simply a linear relationship between P_s^2 and T, a fact which is confirmed by the experimental results in a temperature range of about 10° below the transition point (H 1). The coefficient ξ can then be determined simply from the slope of the P^2 vs. T curve in the vicinity of the transition temperature. The result is: $\xi = 9.3 \times 10^{-10}$ (e.s.u./cm^2)$^{-2}$. The main part of the difference between this value and that reported above is due to the rather wide range of experimental accuracy (10–15%).

There is another method to determine the coefficients of the power expansion (II-1). This method makes use of the nonlinear properties of the dielectric constant near the transition point *in the non-polar phase*. From (II-1), dropping the sixth-order term, we obtain immediately

$$\frac{\partial E}{\partial P} \cong \frac{4\pi}{\varepsilon} = \chi + 3\xi P^2. \tag{II-3}$$

Thus, if one can measure the dielectric constant as a function of polarization in the non-polar state, one has a way to determine ξ. Such measurements were carried out by Triebwasser (T 1) using a method described by Drougard *et al.* (D 2) for the investigation of the polarization dependence of the capacitance of a sample. The experimental arrangement is depicted schematically in Fig. II-6. The capa-

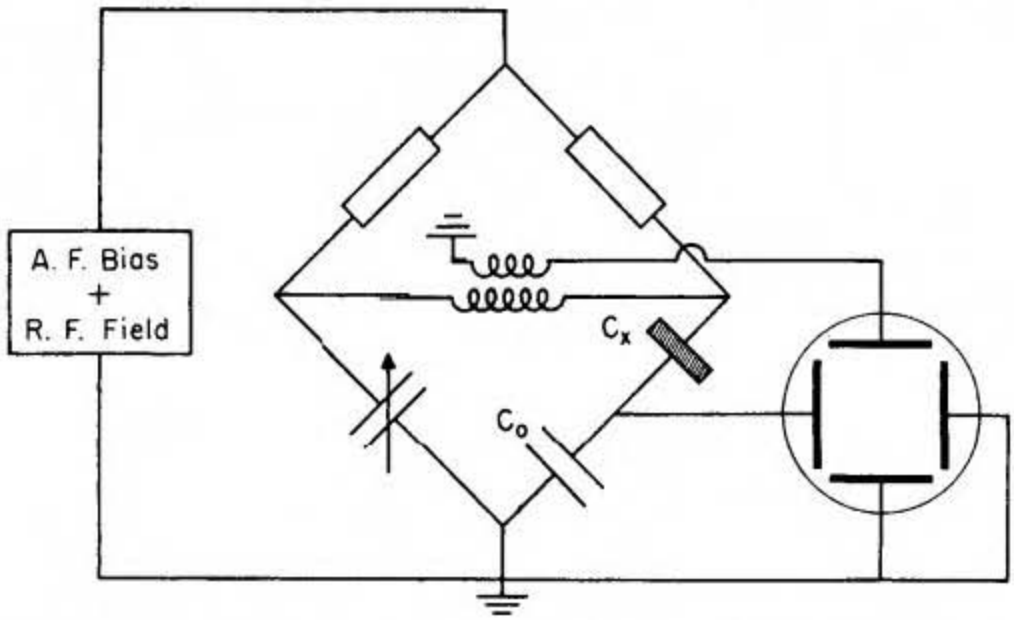

FIG. II-6. Schematic diagram for the investigation of the polarization dependence of the dielectric constant.

citance bridge is fed with a very small-amplitude radiofrequency field (e.g. 50 kc/s) superimposed on a large-amplitude low-frequency field (e.g. 60 c/s). The voltage across the linear capacitor C_0, in series with the crystal C_x, is proportional to the polarization developed across the sample by the biasing low-frequency field, and is applied to the X axis of an oscilloscope. The bridge output is applied to the Y axis of the scope, so that the unbalance of the bridge is displayed against the polarization and the bridge can thus be balanced for any value of the polarization.

The results of Triebwasser's measurements are shown in Fig. II-7. According to Eq. (II-3), the slope of the straight line in this figure yields the value of ξ. The result is $\xi = 9.2 \times 10^{-10}$ (e.s.u./cm^2)$^{-2}$. This value necessitates a correction due to the adiabatic conditions of the measurement (see Section 5), after which the value of ξ becomes equal to 7.7×10^{-10} (e.s.u./cm^2)$^{-2}$, in excellent agreement with the value obtained from the measurements in the polar phase. The con-

sistency of the values of ξ determined above and below the transition temperature is a quantitative confirmation of the applicability of the thermodynamic theory.

The low-frequency biasing field used in the above experiment can be replaced by a d.c. biasing field. The non-linearity of the dielectric constant can thus be determined by measuring the capacitance of the sample with a small a.c. field superimposed on a large d.c. biasing field. The result can be predicted from the free-energy function: given a value of P, we can compute the dielectric constant from (II-3) and the electric field from the partial derivative of the free energy

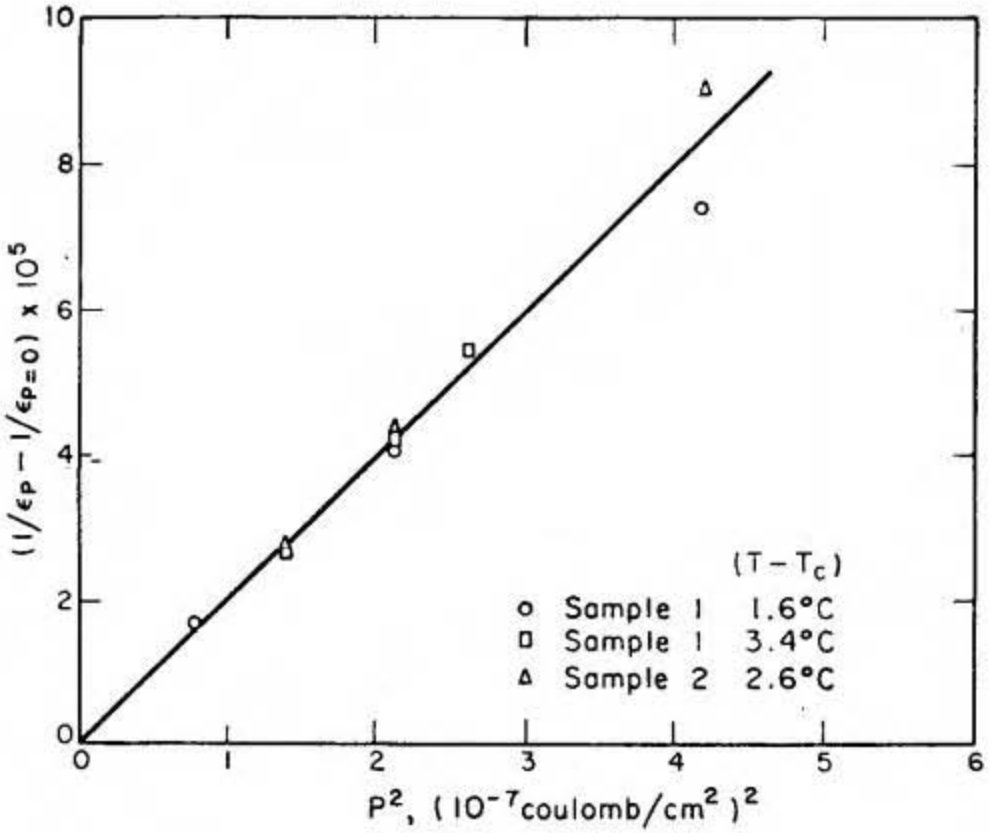

FIG. II-7. Polarization dependence of the dielectric constant of tri-glycine sulfate (biasing field 200 c/s sine wave, measuring field 50 kc/s) (according to Triebwasser (T 1)).

(II-1) with respect to polarization. The result is depicted in Fig. II-8. Measurements of the small-signal dielectric constant under the action of d.c. biasing fields were also carried out by Chapelle and Taurel (C 5). These measurements indicate a small variation of the ξ coefficient with temperature.

4. Specific Heat

The specific heat c_μ of TGS was measured by Hoshino *et al.* (H 1) in the temperature range from 10 to 65 °C, i.e. through the transition point. The experimental results are shown graphically in Fig. II-9, and clearly indicate an anomaly of the specific heat over a relatively wide temperature range in the vicinity of the transition. The shape of the curve is particularly interesting not only because

it is indicative of a second order transition, a fact already established by the dielectric data, but especially because it does not show the characteristics of a λ-type transition.

The heat of transition ΔQ and the corresponding entropy change ΔS can be determined by integrating the experimental curve of the excess specific heat. The results are (H 1)

$$\Delta Q = 150 \text{ cal/mole},$$

$$\Delta S = 0.48 \text{ cal/mole } ^\circ\text{C}.$$

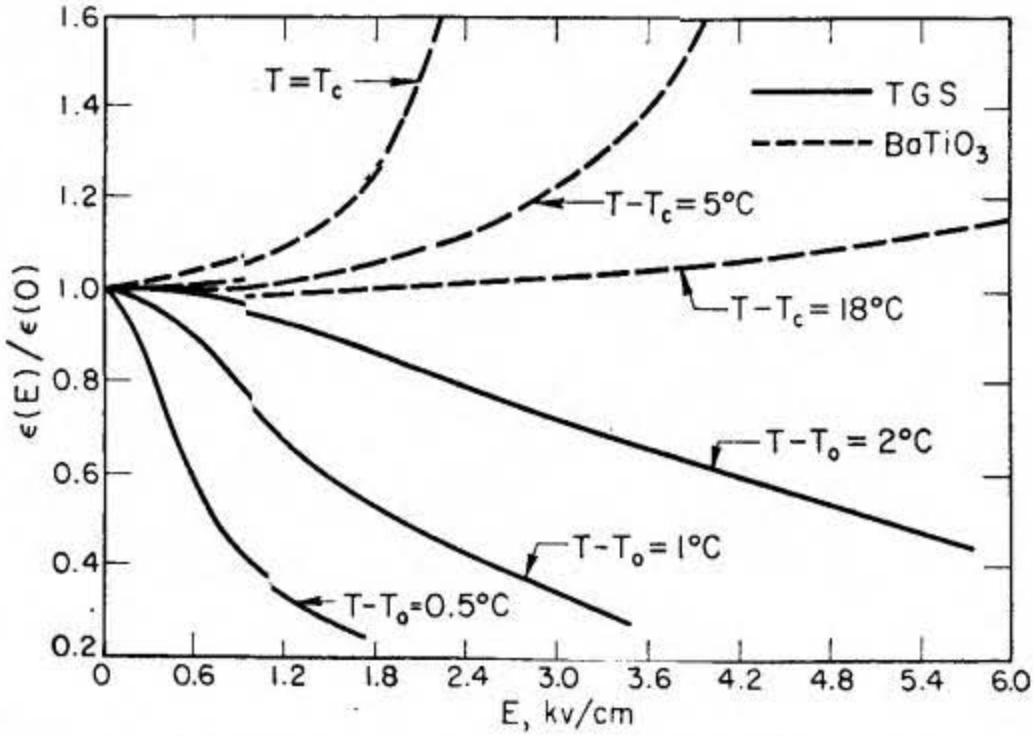

FIG. II-8. Field dependence of the dielectric constant of tri-glycine sulfate. The case of $BaTiO_3$ is also shown as an example of the behavior expected theoretically for a first-order phase change (according to Triebwasser (T 1)).

Let us now see how well these results compare with those expected on the basis of the thermodynamic theory. Since the entropy S is equal to $-(\partial A/\partial T)_P$ and we have assumed that the coefficients ξ and ζ are temperature independent, we obtain for the entropy change:

$$\Delta S = S_0 - S = \frac{2\pi}{C} \Delta P^2, \tag{II-4}$$

where S and S_0 represent the entropies of the polar and non-polar states, respectively. Using the experimental data for the Curie constant and the spontaneous polarization at 23 °C, we obtain

$$\Delta S = 0.64 \text{ cal/mole } ^\circ\text{C},$$

in fair agreement with the above value determined from the specific heat curve. The accuracy involved in this comparison is poor, owing to the fairly small transition energy of TGS, which is strongly affected by the choice of the base line in Fig. II-9.

We can further compute the excess specific heat from Eq. (II-4):

$$\Delta c_p = c_p - c_p^0 = \frac{2\pi}{C} T \frac{\partial P^2}{\partial T}, \tag{II-5}$$

where c_p and c_p^0 represent the specific heats of the polar and non-polar states respectively. Equation (II-5) allows us to compute the expected temperature dependence of c_p from the dielectric data and compare it with the direct measurement (Fig. II-9). It is quite clear that the flat top of the theoretical curve is a consequence of the linear temperature dependence of P^2 in the immediate vicinity of the transition (Eq. II-2). The agreement between the shape of the experimental curve and that calculated from the dielectric data is, however, not quite as satisfactory as one would wish. It has been pointed out (H 1) that the thermodynamic treatment based on the expansion of the free energy in terms of polarization only may be incomplete, as it does not take into account short-range order effects.

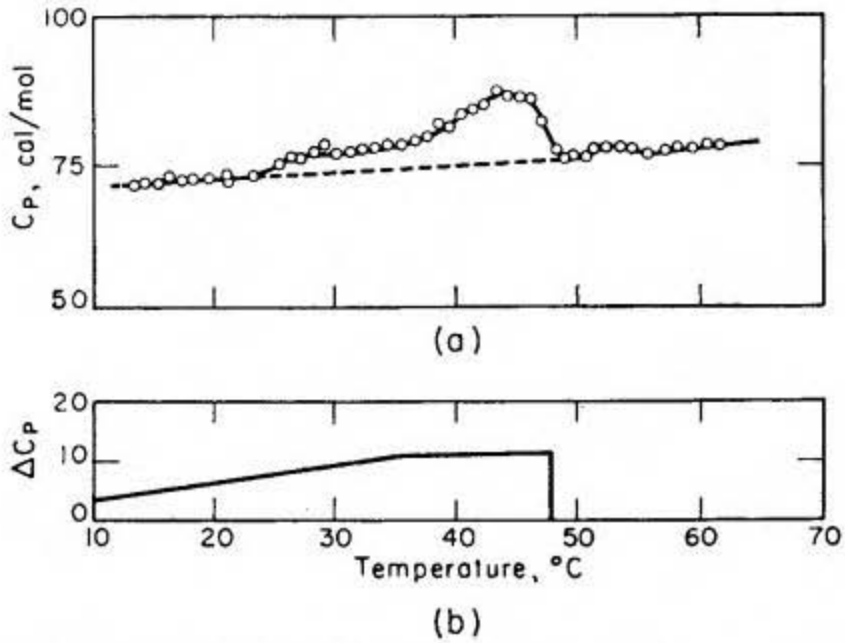

FIG. II-9. Specific heat of tri-glycine sulfate as a function of temperature. (a) Experimental. (b) Theoretical (according to Hoshino *et al.* (H 1)).

5. Adiabatic and Isothermal Dielectric Constant

The fact that the polarization is a rapidly varying function of temperature and field in the vicinity of the transition point has other important consequences, e.g. the differentiation between the values of the dielectric constant measured isothermally and adiabatically.

We have seen in Chapter I that a certain relationship is expected between the dielectric constant below and the dielectric constant above the transition. This relationship, Eq. (I-10), yields the value of the reciprocal dielectric susceptibility $(\partial^2 A/\partial P^2)$ below the Curie temperature and is rewritten here for convenience:

$$\frac{\partial^2 A}{\partial P^2} = 2\chi^X. \tag{II-6}$$

Since the reciprocal dielectric constant is a linear function of temperature above (Curie–Weiss law) as well as below the transition point (Fig. II-3), Eq. (II-6) requires that the downward slope be just *twice* as steep as the upward slope. However, the ratio between the slopes of the experimental lines is found to be 2.7, with an accuracy of about $\pm 10\%$. The reason for this discrepancy is to be sought in the fact that the dielectric constant measured with an a.c. field of, say, 10 kc/s in the ferroelectric range represents an adiabatic value, while the theory assumes isothermal conditions.

In the following, we want to derive an expression relating the adiabatic dielectric constant ε_S to the isothermal dielectric constant ε_T (D 3), (T 1), (W 3). Considering the electric field E as an explicit function of temperature T, entropy S and polarization P, i.e. $E(T, S, P)$; writing the total differential $\mathrm{d}E$ in terms of partial derivatives, and putting $\mathrm{d}S = 0$ for an adiabatic process, we obtain:

$$\left(\frac{\partial E}{\partial P}\right)_S = \left(\frac{\partial E}{\partial T}\right)_P \left(\frac{\partial T}{\partial P}\right)_S + \left(\frac{\partial E}{\partial P}\right)_T. \qquad \text{(II-7)}$$

The partial derivative $(\partial T/\partial P)_S$ can be written in another way as follows. From the expression for the free energy A of a stress-free crystal:

$$\mathrm{d}A = T\mathrm{d}S + E\mathrm{d}P$$

we have $T = (\partial A/\partial S)_P$ and $E = (\partial A/\partial P)_S$, and hence the Maxwell's relation

$$\left(\frac{\partial T}{\partial P}\right)_S = \left(\frac{\partial E}{\partial S}\right)_P,$$

which latter can be written

$$\left(\frac{\partial E}{\partial S}\right)_P = \left(\frac{\partial E}{\partial T}\right)_P \Big/ \left(\frac{\partial S}{\partial T}\right)_P,$$

so that Eq. (II-7) becomes:

$$\left(\frac{\partial E}{\partial P}\right)_S = \left(\frac{\partial E}{\partial P}\right)_T + \left(\frac{\partial E}{\partial T}\right)_P^2 \Big/ \left(\frac{\partial S}{\partial T}\right)_P. \qquad \text{(II-8)}$$

Now, $(\partial E/\partial P)_S = \chi_S$, or the reciprocal adiabatic dielectric susceptibility; $(\partial E/\partial P)_T = \chi_T$, or the reciprocal isothermal dielectric susceptibility; and, finally, by definition, $(\partial S/\partial T)_P = c_P/T$, where c_P represents the specific heat per unit volume at constant polarization P. We can then write Eq. (II-8) thus:

$$\chi_S = \chi_T + \frac{T}{c_P}\left(\frac{\partial E}{\partial T}\right)_P^2. \qquad \text{(II-8a)}$$

The experiment yields the adiabatic value χ_S: how can we compute χ_T by means of Eq. (II-8a)?

It is easy to obtain an expression for $(\partial E/\partial T)_P$ from our free-energy function (II-1) and the previously assumed temperature independence of the coefficients ξ and ζ. We obtain $(\partial E/\partial T)_P = (4\pi/C)\,P$, so that Eq. (II-8) can be written

$$\chi_S = \chi_T + \frac{16\pi^2}{C^2}\,\frac{T}{c_P}\,P^2. \qquad \text{(II-9)}$$

We can correlate this expression with the free-energy expansion (II-1) by noting that $\chi_T = (\partial^2 A/\partial P^2)_T$ and thus, neglecting again the P^6 term of $A(P, T)$:

$$\chi_S = \frac{4\pi}{C}(T - T_0) + 3\xi P^2 + \frac{16\pi^2}{C^2}\frac{T}{c_P}P^2, \tag{II-9a}$$

or since $\chi_S \cong 4\pi/\varepsilon_S$:

$$\frac{1}{\varepsilon_S} = \frac{T - T_0}{C} + \left(\frac{3}{4\pi}\xi + \frac{4\pi T}{C^2 c_P}\right)P^2. \tag{II-10}$$

It may be worthwhile to discuss this expression in more detail:

(i) *Above the transition temperature,* the dielectric constant measured with a *very small* a.c. field is adiabatic in principle, however, in practice we can neglect the correction term as the polarization is also very small. Thus the dielectric constant is characterized by the Curie–Weiss law

$$\left(\frac{1}{\varepsilon}\right)_{T>T_c} = \frac{T - T_0}{C}$$

(first term in Eq. (II-10)). If we apply a biasing field, causing a polarization P, we measure an adiabatic value of the dielectric constant. Thus, the slope of the straight line in Fig. II-7 is equal to the whole expression in the parenthesis on the right-hand side of Eq. (II-10) and the value of ξ can be computed only if the adiabatic correction term is known. The direct measurement of the specific heat at constant pressure reported above (Section 4) yields the value of $c_{E=0}$, i.e. the specific heat at zero field. Above the transition temperature, where $P = 0$ (and also far below this temperature, where the polarization is almost constant), the values of $c_{E=0}$ and c_P are equal and we can thus evaluate the adiabatic correction term, with the results reported in Section 3.

(ii) *Below the transition temperature,* the existence of a spontaneous polarization P_s makes a distinction between adiabatic and isothermal dielectric constant always necessary. In the immediate vicinity of the transition temperature, P_s^2 is given by Eq. (II-2), where we neglect the second-order term. Introducing this expression into (II-10) and arranging the terms we obtain

$$\left(\frac{1}{\varepsilon}\right)_{T<T_c} = -2\frac{T - T_0}{C}\left(1 + \frac{8\pi^2}{C^2 c_P \xi}T\right). \tag{II-11}$$

Differentiating with respect to T, we obtain for the slope of the curve below and near the transition (where $T \approx T_0$):

$$\frac{\mathrm{d}}{\mathrm{d}T}\left(\frac{1}{\varepsilon}\right)_{T<T_c} = -\frac{2}{C}\left(1 + \frac{8\pi^2}{C^2 c_P \xi}T_0\right),$$

while, above the transition temperature:

$$\frac{\mathrm{d}}{\mathrm{d}T}\left(\frac{1}{\varepsilon}\right)_{T>T_c} = \frac{1}{C}.$$

Hence the ratio of the slopes is, in the vicinity of T_0:

$$\frac{\mathrm{d}}{\mathrm{d}T}\left(\frac{1}{\varepsilon}\right)_{T<T_c} \Big/ \frac{\mathrm{d}}{\mathrm{d}T}\left(\frac{1}{\varepsilon}\right)_{T>T_c} = -2\left(1+\frac{8\pi^2}{C^2 c_P \xi} T_0\right). \qquad \text{(II-12)}$$

If we neglect the adiabatic correction term, Eq. (II-12) agrees with Eq. (II-6). Consideration of this term implies a correction of about 20% thus predicting a slope ratio of 2.4, to be compared with the experimental value 2.7 (T 1). The residual discrepancy, which may be outside the range of the experimental error, may be explained by the fact that, below that transition temperature, the crystal consists of many domains polarized antiparallel to each other which may cause partial clamping (H 1). The phenomenon of domain clamping will be discussed in Chapter IV.

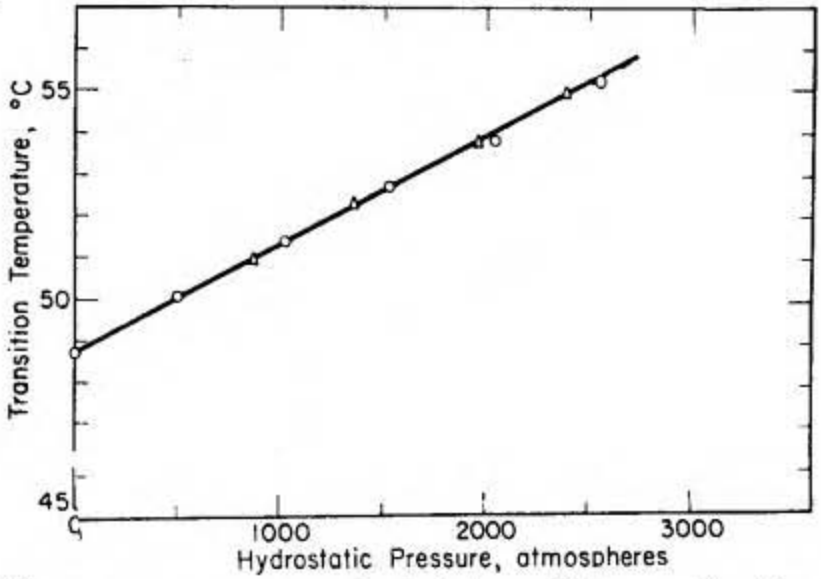

FIG. II-10. Transition temperature of tri-glycine sulfate as a function of hydrostatic pressure (according to Jona and Shirane (J 1)).

6. Effects of Stresses and Radiation

The dielectric properties of ferroelectric crystals can be strongly affected by a number of agents, such as external stresses, fields and radiations. It is interesting to study these effects because they will help to shed light on the microscopic mechanism leading to ferroelectricity. In the case of tri-glycine sulfate, two such effects have been studied in detail, viz., the effect of hydrostatic pressures and that of radiation damage.

Pressure Effects

Application of hydrostatic pressures up to 2700 atm shows that the Curie temperature of TGS is displaced linearly upwards by the pressure p, according to the simple formula(J 1):

$$T_c = T_c^0 + Kp, \qquad \text{(II-13)}$$

where T_c^0 is the transition temperature at atmospheric pressure and $K = 2.6 \times 10^{-3}$ °C/atm (Fig. II-10). All the characteristics of the ferroelectric transition (Curie–Weiss law, onset and value of the spontaneous polarization) remain unaltered with respect to the new transition temperature.

The displacement of the critical temperature T_c with pressure p in the second-order transition of TGS can be predicted according to the well-known Ehrenfest relation (E 1):

$$\frac{\mathrm{d}T_c}{\mathrm{d}p} = \frac{\alpha - \alpha'}{c_p - c_p'} \frac{T_c}{\varrho}, \tag{II-14}$$

where α and α' designate the volume expansion coefficients above and below T_c, respectively; c_p and c_p' the corresponding specific heats at constant pressure and ϱ the density of the crystal.

The same displacement can be predicted, on the other hand, on the basis of the expansion of the free-energy function of stress and polarization, $A(X, P)$, formally similar to expression (I-1). This expansion can be simplified in the present centrosymmetrical case, as the only non-zero components of the stress tensor are $X_{11} = X_{22} = X_{33} \quad p$, and, of course, the only non-zero component of the polarization vector is $P_2 = P$. Thus we obtain the following expression for the free energy in terms of hydrostatic pressure p and polarization P:

$$A(p, P, T) = Sp^2 + KpP^2 + A(P, T),$$

where the quantities S and K are functions of the elastic and electrostrictive constants, and $A(P, T)$ is the free-energy function of polarization P for zero stress [Eq. (II-1)]. Collecting terms, we obtain:

$$A(p, P, T) = Sp^2 + \frac{2\pi}{C}[T - (T_c^0 + Kp)]P^2 + \frac{1}{4}\xi P^4. \tag{II-15}$$

Thus, we can predict that:

(i) The transition temperature depends linearly on the applied hydrostatic pressure p.

(ii) The reciprocal dielectric constant of the non-polar phase follows a Curie–Weiss law even under hydrostatic pressure and the Curie constant is unaffected by pressure.

(iii) An expression for P_s^2 can be obtained from (II-15) which is similar to (II-2), namely:

$$P_s^2 = -\frac{4\pi}{C\xi}[T - (T_c^0 + Kp)].$$

This shows that, in the vicinity of the transition temperature and with the assumption that the coefficient ξ is independent of pressure, the square of the spontaneous polarization is a linear function of both temperature and pressure.

The experiment confirms the above predictions (J 1) within the experimental accuracy, thus justifying the assumptions made for their derivation.

Radiation Effects

Radiation damage effects on TGS have been reported by Chynoweth (C 1) who used 30 keV X-rays as damaging radiation and studied its effect on the hysteresis loops. Small X-ray dosages are reportedly sufficient to cause very

remarkable deformations of the hysteresis loop. Figure II-11 is a typical form assumed by an originally rectangular hysteresis loop; the curve splits into two separate loops, each fairly rectangular, and which are biased by equal and opposite amounts along the field axis. There appears to be no appreciable threshold energy required of the X-rays in order to produce the effects, if the bombardment times

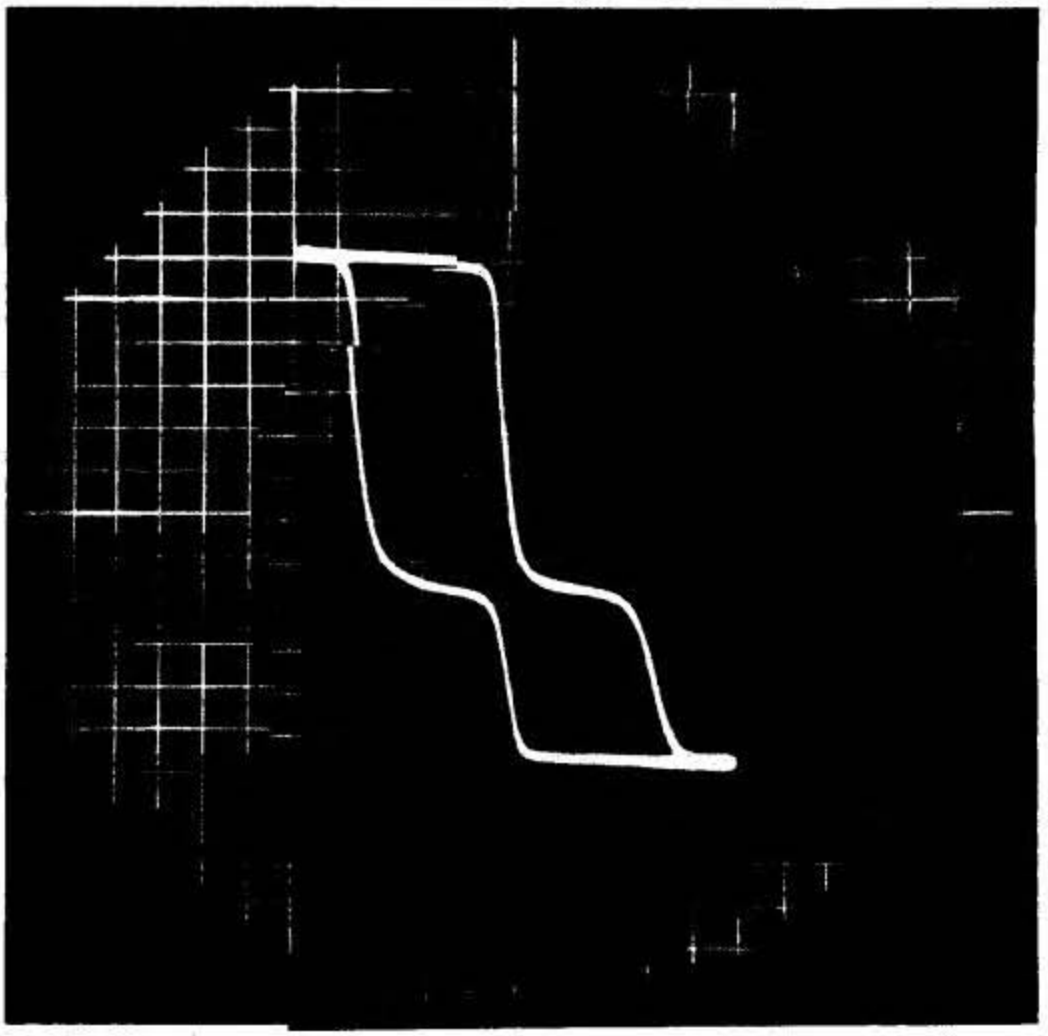

FIG. II-11. Typical distortion of hysteresis loop of tri-glycine sulfate as a consequence of X-ray bombardment (according to Chynoweth (C 1)).

are adjusted accordingly. This suggests that the damage results from effects of ionization rather than from ionic displacements. The effect is also the same irrespectively of whether the crystal is bombarded above or below the transition point, but application of an electric a.c. field during or immediately after the bombardment seems to relieve the distortion temporarily. A diagram showing the pattern of the radiation damage and annealing effects is depicted in Fig. II-12. There is evidence for very severe strain in the crystals exposed to radiation, while the experimental tests seem to deny any explanation of the effects on the basis of space-charge fields.

The detailed origin of the radiation damage effects is not known to date and will have to await more detailed investigations of the effect of radiation

damage on other characteristics of the ferroelectric transition in TGS, such as the dielectric constant, the transition temperature, the elastic constants etc. A tentative explanation has recently been proposed by Abe (A 1) in terms of the strains caused by lattice imperfections due to the radiation. Similar radiation damage effects have been observed in Rochelle salt crystals, using both X-rays

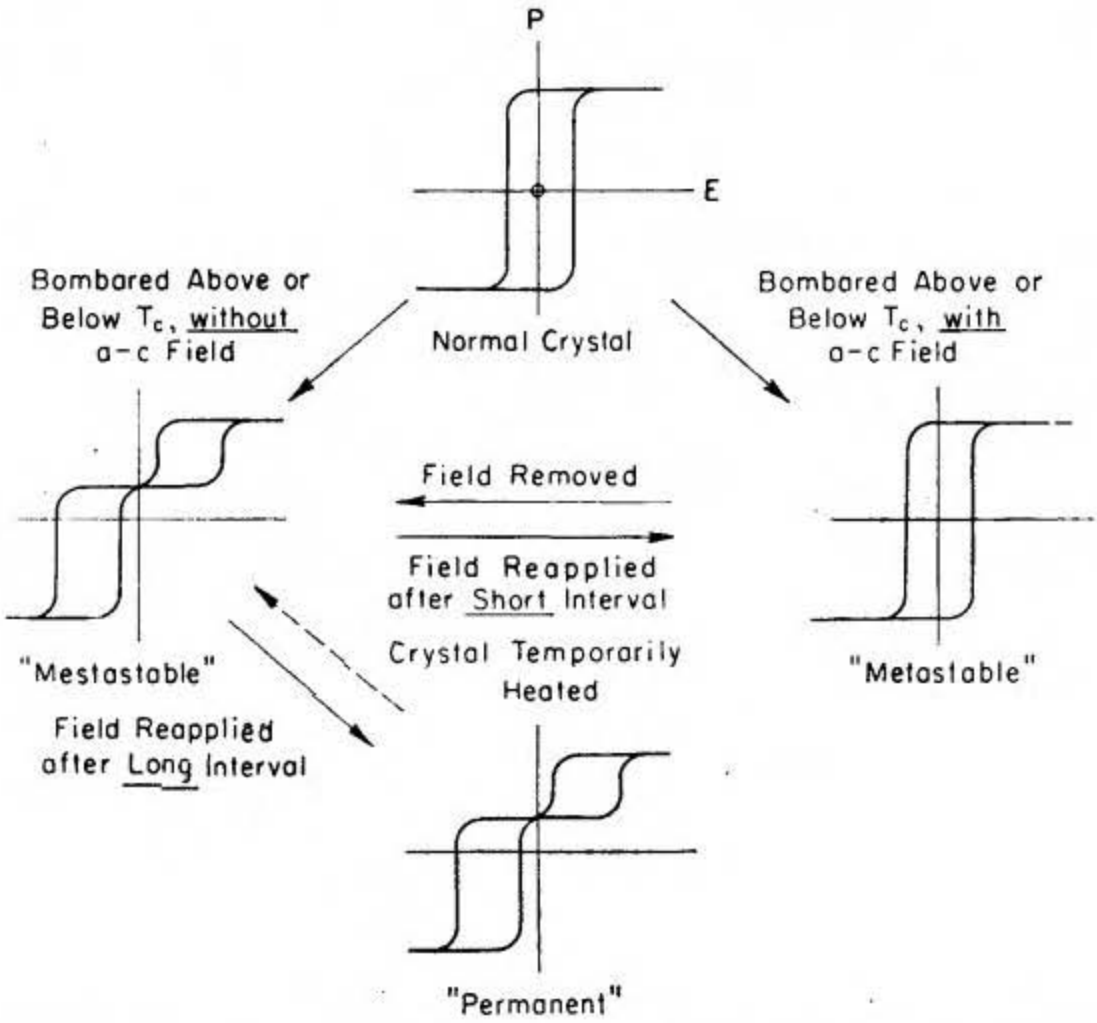

FIG. II-12. Pattern of radiation damage and annealing effects on the hysteresis loop of tri-glycine sulfate (according to Chynoweth (C 1)).

and γ-radiation (see Chapter VII). Unfortunately, we do not know, to date, how much this damage affects the structure of the crystals investigated. If this is the case, an interesting point arising from these investigations is that (C 1), as the X-ray dosages required to produce large changes in the ferroelectric properties are small compared with those normally used in crystallographic structure determinations, there is some doubt whether the structure determined by X-ray crystallography (see Section 9) represents the structure of an undamaged tri-glycine sulfate crystal.

The effect of neutron bombardment upon the dielectric properties of TGS has been recently investigated by Fatuzzo (F 5).

7. Domains

General Considerations about Ferroelectric Domains

In an ideally perfect ferroelectric crystal, the existence of domains can be understood on the basis of qualitative energetic considerations. Suppose that we start from a perfect, non-conducting, insulated ferroelectric crystal in vacuum, which is required to have a uniform spontaneous polarization throughout. For the sake of simplicity, we assume that the shape of this hypothetical "single-domain" crystal is spherical. Then the charges induced on the external surfaces will create a depolarizing electric field whose energy is proportional to the volume of the crystal and the square of the polarization. Such a depolarizing field makes it impossible for the crystal to remain in the uniformly polarized state hypothesized initially. The result is a destruction of the uniform polarization: the crystal is consequently subdivided into regions, or domains, having antiparallel directions of spontaneous polarization, a state which is energetically more stable because it reduces the depolarizing field. This process, however, will not proceed indefinitely, because a certain amount of energy is going to be stored in the boundary layers, or "walls" between the domains. When the overall wall energy has increased to the point of balancing the decrease in energy of the depolarizing field, then an equilibrium configuration is reached and this is going to be the stable domain configuration at the temperature considered.

This, however, is only true if the crystal is ideally *perfect*. In a *real* crystal, the domain configuration resulting from the energetic balance mentioned above is hardly stable at any temperature. A real crystal is never an ideal insulator: the charges induced by the spontaneous polarization are partially compensated by bulk and surface conductivity. Furthermore, a real crystal contains a relatively large number of vacancies, dislocations, impurities, in one word, imperfections, which disturb the uniformity of the polarization and, therefore, of the depolarizing field. Finally, most crystals are in a state of non-uniform strain as a consequence of the conditions of the growth process. Therefore, the domain configuration actually observed in a given crystal is the result of a compromise between the energetic requirements of an ideally perfect crystal and the perturbing effects of conductivity, strain and imperfections in a real crystal. The latter effects may proceed very slowly with time, and therefore the observed domain configuration of a real crystal may be only metastable (aging effects).

In addition, it should be emphasized that one of the most important factors affecting a given domain pattern in a real crystal is the way in which the domains are created when the crystal is cooled through the Curie temperature. The process of domain formation at this temperature involves nucleation. This is most important for crystals which undergo a transition of the first order but may also play an important role in those which undergo a second-order transition, if the temperature distribution throughout the crystal is non-uniform. As the nucleation process is also dependent on strains and imperfections, the domain pattern which is formed at first does not always correspond to an absolute minimum of the free energy. This state is only metastable.

The theoretical calculation of the domain wall energy is a very complicated problem that can be solved only in special simple cases, and connected with it is the problem of the thickness of the domain wall. Again, rather simple energetic considerations are sufficient to convince one that the wall is going to be thin. This is in striking contrast with the situation occurring in ferromagnetic crystals, where the domain wall consists of a transition region in which the magnetization vector turns over gradually from a given direction to the opposite one (see Fig. II-13a). This is so because the thickness of a ferromagnetic domain wall is a result of the compromise between the exchange energy and the anisotropy energy. The former would require a domain boundary as wide as possible, the latter attempts to do just the contrary, in order to avoid the directions of "hard magnetization", but the exchange term is orders of magnitude larger than the

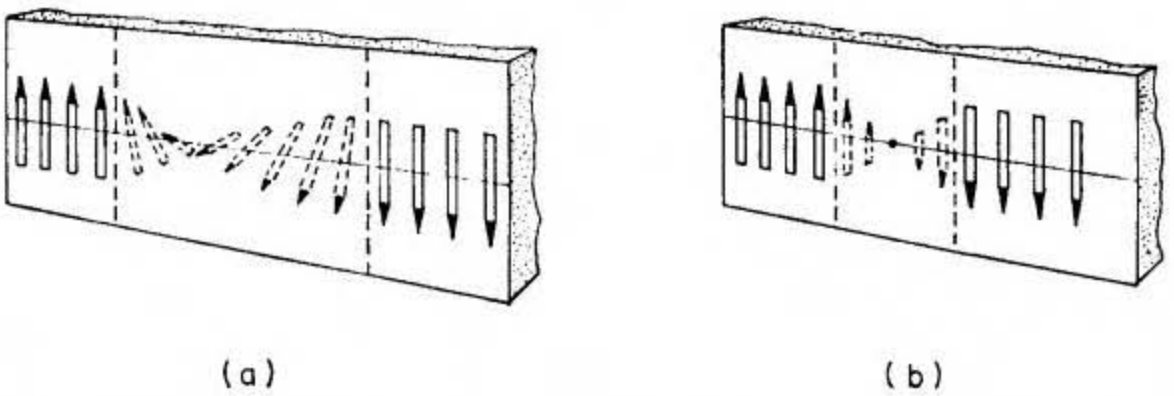

FIG. II-13. Difference between ferromagnetic and ferroelectric 180° domain walls (schematic).
(a) Ferromagnetic wall. In iron, the thickness of the transition layer (comprised between dashed lines) is approximately 300 lattice constants.
(b) Ferroelectric wall. In most ferroelectrics, the thickness of the wall is of the order of one lattice constant.

anisotropy term and the result is a rather thick domain wall. In ferroelectric crystals, there is no real counterpart of the magnetic exchange energy. The polarization may be ionic or electronic, and the main role is played by the electrostatic interaction between polarized ions. We have already mentioned in Chapter I that in a ferroelectric crystal the interaction energies of parallel and antiparallel dipole arrays do not differ much from each other, thus allowing a narrow domain wall. Moreover, the anisotropy of most ferroelectrics, especially those with low symmetry like TGS, is so high that the direction of the spontaneous polarization can hardly deviate from that of the ferroelectric axis. Hence, the polarization vector will not rotate within the wall, but rather will decrease in magnitude, passing through zero, and increase on the other side with opposite sign (see Fig. II-13b). The elastic energy plays also an important role, owing to the strain caused by the polarization through the piezoelectric effect, and this contribution will also favor, in general, a rather thin domain wall.

We can only hope to learn more about the factors causing the domain configuration actually observed in a ferroelectric crystal from a direct study of the

ferroelectric domains. Such a study involves the observation of the geometry of the domains, i.e. their static properties, and the direct or indirect observation of the motion of the domains, i.e. their kinematic characteristics. The former can be carried out with optical or X-ray methods, the latter both with optical and electrical means.

The Geometry of Domains in TGS

The ferroelectric domains of TGS cannot be observed directly under the polarizing microscope, as long as the investigated sample is unstrained. This is due to the fact that the symmetry of the non-polar phase is centrosymmetric (non-piezoelectric), so that the (electrostrictive) strain caused by an electric field along the *b* axis remains the same, in magnitude and sign, when the field is reversed. Polarization reversal changes the crystal from a right-handed to a left-handed one, or vice versa, but does not displace the optic plane (S 1), (T 6).

The domains can, however, be suitably identified by means of etching techniques. This method, which was first applied to the study of ferroelectric domains by Hooton and Merz (H 2) on barium titanate (see Chapter IV), makes use of the well-known fact that the two ends of a polar axis have different properties. Thus, the dissolving (etching) rate of the positive end ("head") of the polar axis is different from that of the negative end ("tail") of the same axis. Clearly, this method enables us only to study the *surface* of a TGS plate cleaved perpendicularly to the polar axis, but we can, in this way, see how large the cross section of the domains is.

The effects of various etchants, such as water, methanol, acetone etc., on TGS plates have been reported by Toyoda and co-workers (T 4), (T 6), (T 7), who established that the positive end of the polar axis etches faster, and thus appears uneven, than the negative end which, therefore, has a smooth appearance. Figure II-14 shows a photograph of the etch patterns obtained by Konstantinova *et al.* (K 2) on the top and bottom surfaces of a thin plate of TGS cut perpendicular to the polar axis. One pattern is the mirror image of the other, showing that most of the domains penetrate throughout the crystal. The cross-sectional dimensions vary from a few-tenths of a millimeter to several millimeters. The polarity of adjacent domains can be checked with an electrometer, thus establishing that the sign is reversed in going from one domain to the adjacent one. The cross-section is mostly oval shaped and irregular.

A detailed investigation of domain patterns in TGS has been recently carried out by Chynoweth and Feldmann (C 6) using water as an etchant. The technique consists in immersing the polished sample in water for periods of time varying from a few to several seconds, depending on the temperature of the water bath. Despite its obvious limitations due to the high solubility of TGS in water, this technique has the advantage of a markedly high resolution in revealing fine details of the domain structure. As already indicated by the photograph in Fig. II-14, the small domains appear to have most frequently elliptical or lenticular shape, the major axes of the ellipses lying approximately in the direc-

tion of the optic plane (Fig. II-15a). Only the larger domains appear to run through the crystal from one surface to the other, but the domain walls are not always exactly parallel to the ferroelectric axis. The smaller domains terminate within the crystal plate in the form of spikes. This has been verified by etching the side of the crystal parallel to the ferroelectric axis and is shown in the photomicrograph of Fig. II-15(b). It is, incidentally, rather surprising, at first, to see that domains can be revealed in this way, as the polarization for either sign

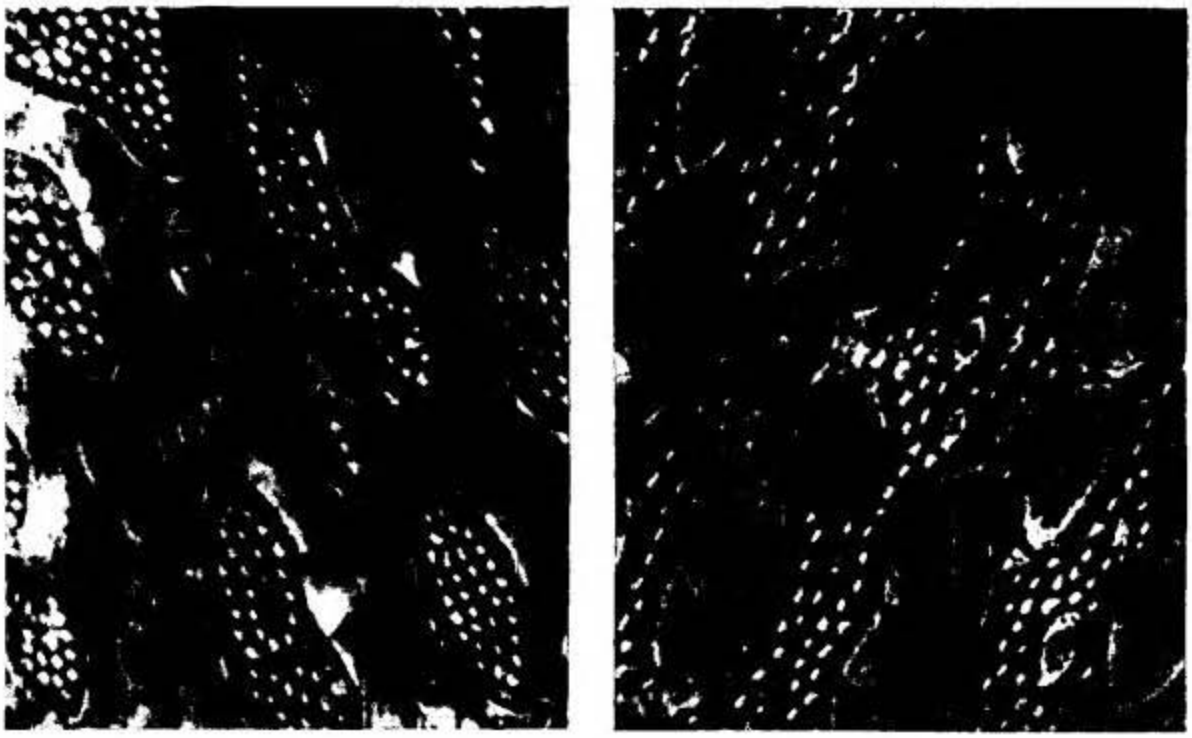

FIG. II-14. Photograph of the etched top and bottom surfaces of a plate of tri-glycine sulfate perpendicular to the polar axis (according to Konstantinova *et al.* (K 2)).

of domain is supposedly parallel to the surface. However, this fact may possibly be understood on the basis of the structural mechanism involved in the reversal of polarity (see Section 9). This technique of etching the side of the crystal confirms the fact that the larger domains run right through the crystal and, in addition, reveals often domains which are completely internal. As shown in Fig. II-16(a), these internal domains appear as long, thin, cigar-shaped regions pointed at both ends, lying along the ferroelectric axis, and are most probably lenticular in cross-section.

Chynoweth and Feldmann (C 6) were able to show that very regular arrays of domains are introduced into the crystals when they are subjected to thermal shocks. A cooling shock gives rise to many small spike-shaped nuclei extending into the crystal from the surfaces. A warming shock results in a regular array of considerably larger domains. The following model was proposed to account for the observed phenomena. Consider a non-electroded crystal plate initially in thermal equilibrium at the temperature T_1 and then subjected to a sudden cooling shock to a temperature $T_2 (T_2 < T_1)$. Obviously, the surface of the

plate will be the first to attain the new temperature T_2, and there will be a more or less sharp temperature boundary moving rapidly into the interior of the crystal plate. Owing to the temperature difference across the boundary there will be a

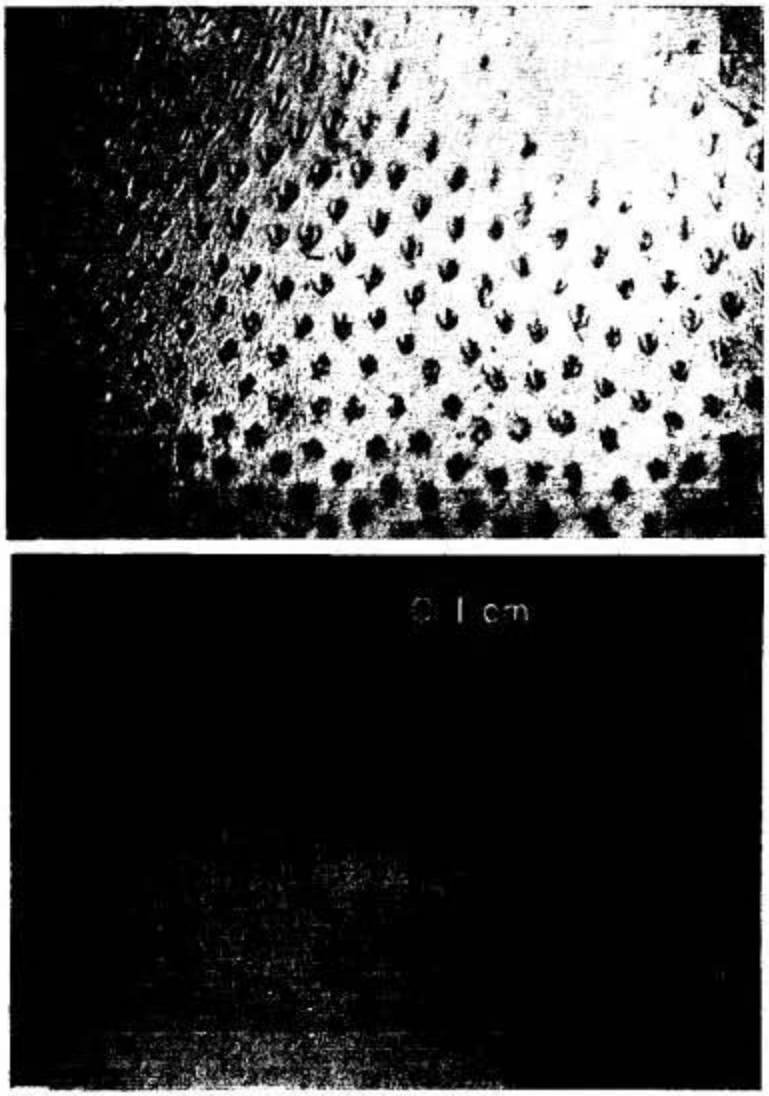

FIG. II-15. Fine detail of domain pattern of tri-glycine sulfate as revealed by the water-etching technique.
(a) Face perpendicular to the ferroelectric axis,
(b) Face parallel to the ferroelectric axis.
The photographs show that the fine dots in (a) represent the basis of small spike-shaped domains (according to Chynoweth and Feldman (C 6)).

discontinuity in the spontaneous polarization. The polarization discontinuities give rise to bound charges which will be compensated to some extent by free charges external to the crystal. These charges, in turn, give rise to fields both in the regions between the crystal surface and the temperature boundary, and in the interior of the plate between the two temperature boundaries. It is easy to see that the former fields oppose the polarization and so will cause domains to nucleate at the crystal surfaces; the latter fields (in the interior) are in the same direction as the polarization and so will not give rise to reverse polarized domains. In the warming shock, however ($T_2 < T_1$), by a similar argument the

fields in the surface regions will be in the same direction as the polarization, but in the interior the field will oppose the polarization and so can cause the nucleation of internal domains. Under the influence of the interior field these domains will tend to grow often as far as the surface of the crystal plate (C 6). This model

FIG. II-16. Ferroelectric domains in tri-glycine sulfate as revealed on a side of the crystal parallel to the ferroelectric axis, (a) by the water-etching technique, (b) by the powder deposition method. Note that each of the domains in (a) correlates with a domain in (b) but there are also many others in (b) which do not show in (a). This demonstrates the ability of the powder technique to reveal domains submerged below the crystal surface (according to Chynoweth and Feldman (C 6)).

seems to provide a satisfactory qualitative explanation for the domain patterns observed experimentally after thermal shocks.

Another technique for delineating ferroelectric domain patterns was reported by Pearson and Feldmann (P 2) and applied, among other crystals, to TGS. The technique consists in using a colloidal suspension of electrostatically charged powders in insulating organic liquids. It is found that yellow sulfur suspended in hexane deposits best on negative dipole ends, while red lead oxide deposits satisfactorily on positive dipole ends. The "powder patterns" of domains are

obtained by placing a few drops of colloid solution on the crystal surface. After the hexane has evaporated, the powders are fixed in place indefinitely by the electrostatic charges. Figure II-17 shows a comparison between the results obtained with the powder technique (Fig. II-17a) and those obtained with the etching technique (Fig. II-17b). The correlation between the two patterns is complete. Figure II-16(b), on the other hand, shows that the powder deposition technique can also be successfully applied to the study of internal domains that do not cross the surface of (010) plates.

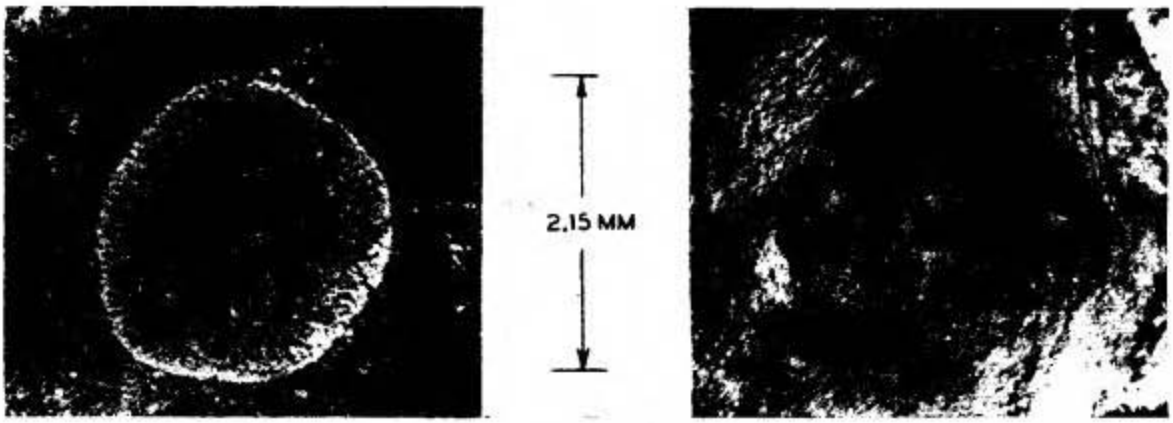

FIG. II-17. Comparison of powder and etch patterns on tri-glycine sulfate crystals. (a) Sulfur powder, (b) Same crystal etched in water. Circular areas are negative domains (according to Pearson and Feldman (P 2)).

The Process of Polarization Reversal

It is quite evident that when the polarization of a ferroelectric crystal is reversed by means of an external electric field, the domain configuration must undergo radical changes. It has therefore become customary to speak of either polarization reversal, dynamic properties of the domains, or switching characteristics, when referring to the same physical process, namely the way in which polarity is reversed by an external field. A large amount of work has been done on various ferroelectrics, including TGS, in order to understand this process. Most of the methods of investigations have been developed for the work on $BaTiO_3$ (see Section IV-8), and subsequently applied to other ferroelectrics. These methods may be classified roughly into two main groups, viz. (i) direct observation of the motion of domain walls during polarization reversal, and (ii) measurement of the switching transient under pulsing conditions.

Investigations of the latter type have been carried out on TGS by Wieder (W 1), Fatuzzo (F 1), Pulvari and Kuebler (P 3), Toyoda *et al.* (T 3), Kiyasu Zen'iti *et al.* (Z 1) and Fatuzzo and Merz (F 2). The technique mostly employed is that first developed by Merz (M 2) for similar investigations on barium titanate. This technique consists in applying to the crystal a train of rectangular voltage pulses of successive opposite polarities in such a way that each pulse reverses the sign of the previous remanent polarization. The rise time of the pulses must be short (of the order of 10 mμ/sec) as compared to the time required for the field to reverse the polarization of the sample. The amplitude and the duration

of the pulses must be sufficiently large to cause the amount of reversed polarization to be substantially $2P_s$. Finally, the intervals between pulses must be long enough for the crystal to reach an equilibrium state between successive pulses. The pulses are applied to the crystal in series with an ohmic resistance, and the switching current transient developed across this resistance is displayed on an oscilloscope. Figure II-18 shows the switching transient observed under these conditions and defines the switching time t_s as the time required for the switching current to drop to zero. The faster the dipoles switch, the larger the peak current i_{max}.

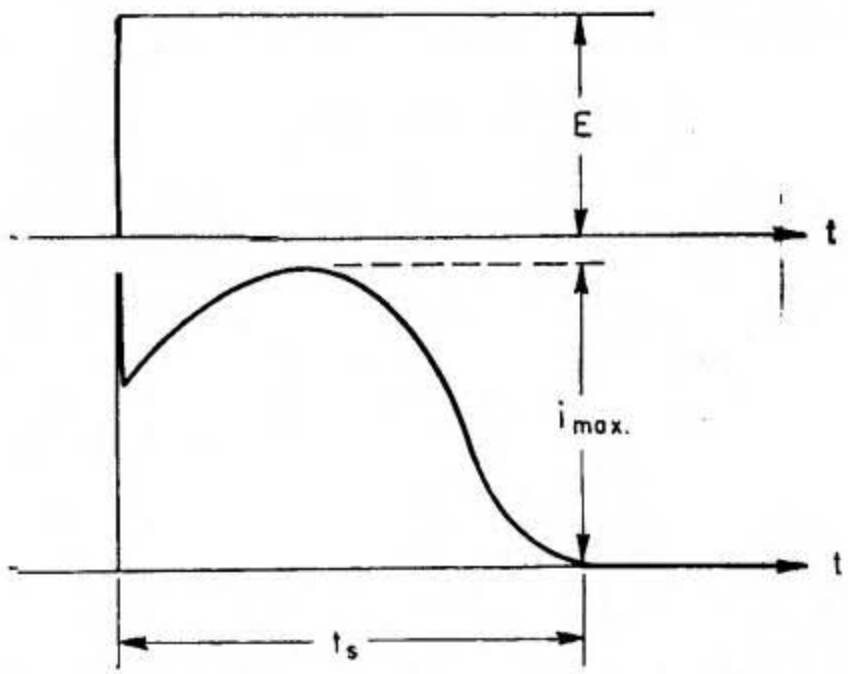

FIG. II-18. Pulsing field and pulsing current as functions of time (schematic).

Figure II-19 shows a plot of the reciprocal of the switching time t_s in TGS as a function of field (F 2). A similar figure can be obtained by plotting the peak current i_{max} as a function of field (W 1). The figure shows that there are three regions of different behavior of the crystal, depending on the applied field. At low field strengths (smaller than about 7 kV/cm) the switching time t_s follows an exponential law of the form

$$\frac{1}{t_s} = \frac{1}{t_\infty} e^{-\alpha/E}, \tag{II-16}$$

where the activation field α is a function of temperature: at 30 °C, $\alpha = 3.8$ kV/cm (W 1). At higher fields the switching mechanism seems to change: we find a linear behavior of $1/t_s$ (and i_{max}) with E:

$$\frac{1}{t_s} = \text{constant} \times E. \tag{II-17}$$

These results can be interpreted in terms of two mechanisms responsible for the switching process: nucleation of domains, and domain wall motion. Following Fatuzzo and Merz (F 2), we define the nucleation time t_n as the time

necessary to form all nuclei, and the domain wall motion time t_d as the time necessary for one domain to grow through the sample. Then, we can write that the total switching time is approximately given by

$$t_s \cong t_n + t_d. \tag{II-18}$$

Thus, if the two quantities t_n and t_d are not of the same order of magnitude, the switching time t_s is determined principally by the slower of the two mechanisms.

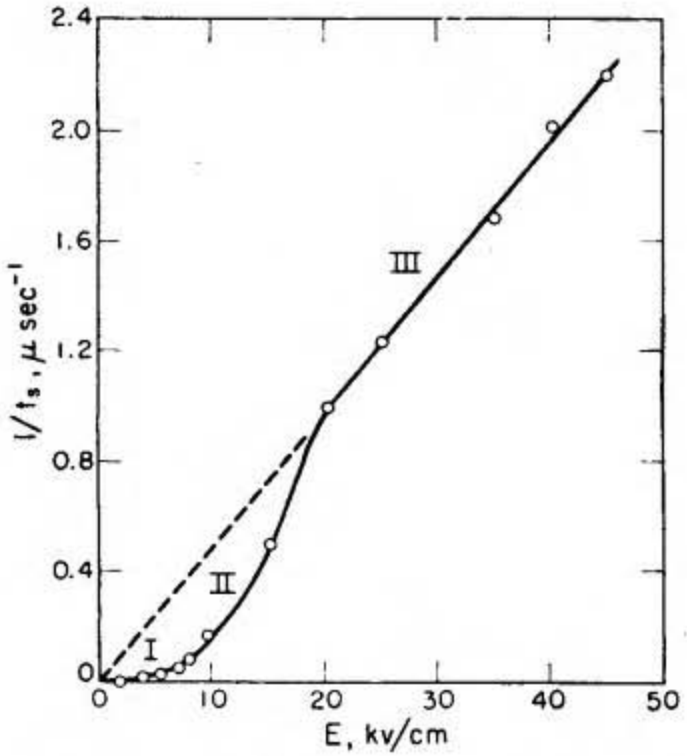

FIG. II-19. Reciprocal switching time t_s of tri-glycine sulfate as a function of field (according to Fatuzzo and Merz (F 2)).

At low fields (region I in Fig. II-19), the rate of nucleation is so low that the switching is primarily governed by nucleation of new domains ($t_n \gg t_d$). Assuming that, at low fields, the probability of forming new domains depends exponentially upon the applied field, thus:

$$p_n = p_0 e^{-\alpha/E}, \tag{II-19}$$

it follows that

$$\frac{1}{t_s} \cong \frac{1}{t_n} = \frac{1}{t_\infty} e^{-\alpha/E}. \tag{II-20}$$

At high field strengths, on the other hand (region III of Fig. II-19), the nucleation rate is so large that the switching time is primarily determined by the velocity of the domain walls ($t_d \gg t_n$). Assuming that the domain wall motion can be described by (F 2):

$$v = \frac{d}{t_d} = \mu E \tag{II-21}$$

where d is the distance covered by the wall in motion (thickness of the sample), and μ the mobility, we obtain

$$\frac{1}{t_s} \cong \frac{1}{t_d} = \frac{\mu}{d} E = \frac{\mu}{d^2} V. \tag{II-22}$$

This implies that, in this region of high fields, the switching time should depend quadratically upon the thickness of the sample, a dependence that was confirmed by the experimental results of Fatuzzo and Merz for applied fields larger than about 10^4 V/cm. The mobility $\mu(T)$ can be determined as a function of temperature from graphs such as Fig. II-19 plotted for different temperatures. At 30 °C, $\mu = 2.2$ cm²/Vsec (W 1). The temperature dependence of the reciprocal mobility $\beta = 1/\mu$ is depicted in Fig. II-20. The rapid increase of β below about -10 °C

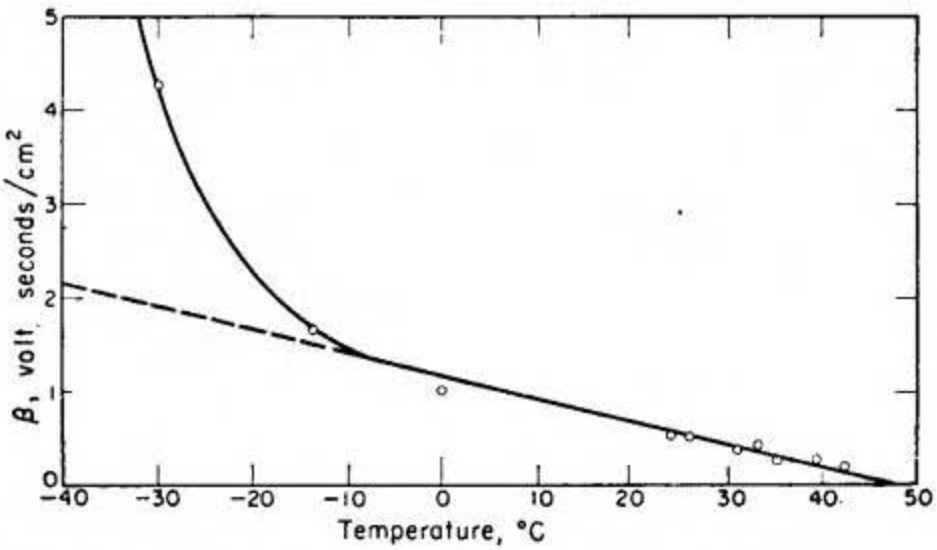

FIG. II-20. Reciprocal mobility $1/\mu = \beta$ in tri-glycine sulfate as a function of temperature (according to Wieder (W 1)).

may be compared with the analogous behavior of the coercive field at these temperatures (Fig. II-5). If the domain wall mobility μ is independent of the applied field, then the observed quadratic dependence of the switching time upon crystal thickness indicates that, at high fields, the forward motion of the domain walls is very much faster than any sidewise motion.

At low fields, on the other hand, sidewise expansion of the nucleated domains may bring a considerable contribution to the switching transient. This has been established by Chynoweth and Abel (C 2) using fields of the order of 30–35 V/cm on specimens provided with liquid electrodes (a saturated solution of TGS and sodium sulfate in normal octyl alcohol), rather than noble metal electrodes. The domains were observed, after any suitable electrical treatment of the sample, by means of the powder deposition technique described above. The experiments proved that, in the field range indicated above, polarization reversal in TGS is usually accomplished by the formation and sideways expansion of a few domains; in some extreme cases, switching was found to occur by the sideways growth of a single domain. The mechanism by which such a sidewise motion

of the wall can occur is not completely understood, at this stage, but there are indications that it may be the result of a continuous formation of new nuclei along the edges of a switched region (C 2), (F 2). This, in turn, may indicate that the probability of formation of new nuclei is affected by the number of growing and already grown domains, an effect that has been called the "nucleus domain interaction" by Fatuzzo and Merz (F 2), and seems to play a role in all ferroelectric reversals, moderate in TGS, very important in $BaTiO_3$ (see Section IV-8), and $LiH_3(SeO_3)_2$ (see Section VIII-8).

It would seem reasonable to expect that the sites at which new domains are nucleated could be predetermined by locally increasing the applied field or decreasing the coercive strength. However, it was proved by Chynoweth and Abel (C 3) that this is not the case. Local increase of the applied field could be achieved by sandblasting small dimples on one surface of the sample; local decrease of the coercive force could be attained by locally damaging a poled crystal with X-rays (C 1). In neither case was it possible to predetermine the nucleation sites at low applied fields. It appears, therefore, that these sites are primarily determined by singularities that are somehow built into the crystal. They seem to have a stronger influence on domain nucleation than the local singularities produced artificially, and are to be considered the cause for the observed reproducibility (C 2) of the domain patterns of crystals that have been alternatively switched partially and totally. It is not possible to say, at this stage, just what these built-in singularities are, but there are reasons to believe that they may be more concentrated on the surface of the sample. In fact, Fatuzzo and Merz (F 2) were able to conclude, from studies of the effect of inhomogeneous temperature changes upon the shape of the switching transients, that heating of the surface alone accelerates the nucleation of new domains, whereas heating of the bulk of the crystal enhances the domain wall motion. It has been suggested (W 1) that the nucleation sites may be crystal imperfections and, as such, may vary in number from sample to sample. Wieder (W 1) has in fact found variations of the value of the activation field α up to 50% in different crystals.

The model of a switching mechanism based upon nucleation and growth of antiparallel domains was investigated in detail by Fatuzzo and Merz (F 2). The nucleated domains grow through the thickness of the crystal in the form of cones until the apices reach the opposite electrode. At this point the walls become perpendicular to the electrode surfaces and the domains assume a more cylindrical shape. Sideway expansion is thereafter aided, most probably, by the nucleus domain interaction which enhances nucleation adjacent to an already existing wall. An analytical treatment of this model let Fatuzzo and Merz (F 2) to satisfactory agreement between calculated and observed switching transients in TGS.

8. Piezoelectric and Elastic Properties

Elastic and piezoelectric measurements of TGS crystals were carried out at room temperature by Konstantinova *et al.* (K 1), who reported complete sets of the elastic constants, elastic compliances and piezoelectric moduli. A partial list

of values of these coefficients was also published by Husimi and Kataoka (H 3). There appears to be no agreement among the values reported by different authors. Husimi and Kataoka (H 3) do not specify the reference system of co-ordinates used in their work, and it is possible that it may differ from that assumed by Konstantinova *et al.* (K 1). However, the discrepancies between the published values of the piezoelectric modulus d_{22}, and those of the elastic compliances s_{22} seem to indicate that the disagreement is likely to be due to causes other than axial choice. In no case is it specified, for example, whether the elastic quantities reported represent constant-field or constant-polarization values. The temperature dependence of some of the piezoelectric moduli d_{ik} was found to be strongly anomalous at the Curie point (H 3).

9. Structural Characteristics

Crystallographic data for tri-glycine sulfate, $(NH_2CH_2COOH)_3 \cdot H_2SO_4$, were reported by Wood and Holden (W 2) as follows:

$$a' = 9.15\ \text{Å}; \quad b' = 12.69\ \text{Å}; \quad c' = 5.73 \pm 0.03\ \text{Å}; \quad \beta = 105°\,40' \pm 20'.$$

The space group, at room temperature, is $C_2^2 - P2_1$ and the experimental density $\varrho = 1.69\ \text{g cm}^{-3}$. There are two formula units in the unit cell. The crystal is optically negative, with $2V = 40 \pm 5°$. The optic plane is almost parallel to the $(\bar{1}02)$ plane. The refractive indices are 1.59, 1.49, 1.56, respectively (T 5).

A detailed structural investigation of the polar room-temperature phase was carried out by Hoshino *et al.* (H 4) using three-dimensional X-ray diffraction data. The axial settings selected for this work,

$$a = 9.42\ \text{Å}; \quad b = 12.64\ \text{Å}; \quad c = 5.73\ \text{Å}; \quad \beta = 110°\,23',$$

are related to those reported above by the transformation formulas:

$$\boldsymbol{a} = \boldsymbol{a}' + \boldsymbol{c}', \quad \boldsymbol{b} = \boldsymbol{b}', \quad \boldsymbol{c} = -\boldsymbol{c}'.$$

A projection of the structure along the c axis is given in Fig. II-21.

The understanding of this structure may be facilitated by a preliminary discussion of the crystal–chemical characteristics of the glycine molecule, NH_2CH_2COOH. When pure glycine crystallizes in its most common modification, the molecular groups assume the so-called zwitter-ion structure, which is commonly written in the form $NH_3^+CH_2COO^-$ to indicate the simultaneous occurrence of positive and negative charges at different points of the molecular group. Furthermore, it is found that the two carbon and the two oxygen atoms lie all in the same plane, while the nitrogen atom is displaced out of the plane (M 3). This is, however, not the only configuration assumed by the glycine group in crystals. It is possible to encounter structures in which the carbon, oxygen and nitrogen atoms are coplanar. For example, the structure of di-glycine chloride shows that both configurations of the glycine group are present in this crystal: the completely planar configuration and the partially planar configuration (with the nitrogen atom displaced from the plane containing the remaining four atoms) (H 5).

Now, the structure of TGS shows that, of the three glycine groups contained in the assymmetric unit (designated with the symbol *A* in Fig. II-21), two assume a completely planar configuration and one assumes the partially planar configuration. In Fig. II-21, the glycine groups designated with I and III are completely planar, the glycine group designated with II is only partially planar: the nitrogen atom is displaced from the plane of the two C's and the two O's of the same group by 0.27 Å. Furthermore, the completely planar groups are

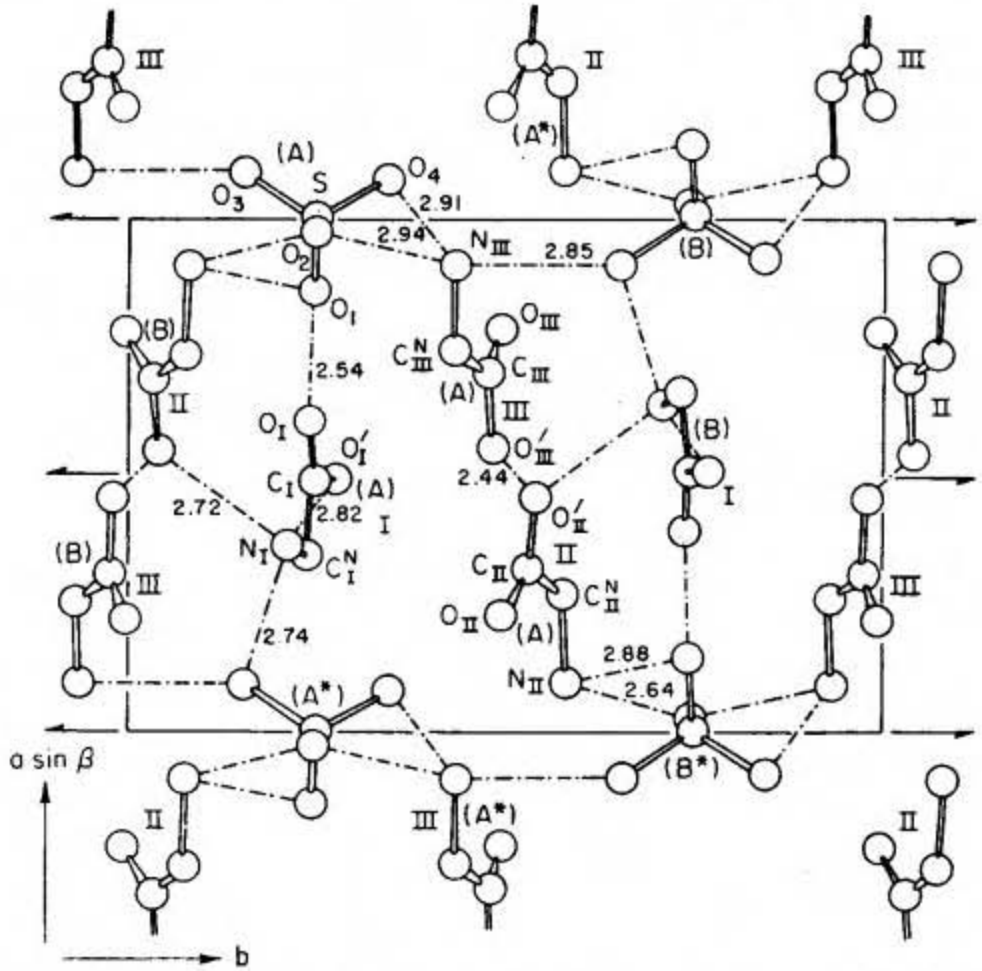

FIG. II-21. Projection of the structure of tri-glycine sulfate along the *c* axis (according to HOSHINO *et al.* (H 4)).

monoprotonated, having taken the protons from the H_2SO_4 group, and are thus best designated as glycinium ions, whereas the partially planar glycine group assumes the zwitter-ion configuration. For this reason, Hoshino *et al.* (H 4) propose to call the compound glycine di-glycinium sulfate and describe it with the chemical formula $(NH_3^+CH_2COO^-)(NH_3^+CH_2COOH)_2 \cdot SO_4^{2-}$.

The molecular plane of the completely planar glycinium ions I makes an angle of 12.5° with the plane at $b = 1/4$. This plane (and that at $b = 3/4$) becomes a crystallographic mirror plane above the Curie temperature, but only statistically, due to random orientation of the glycinium ions I.

As far as the rest of the structure is concerned, the X-ray data indicate a distortion of the sulfate ion from tetrahedral symmetry, at room temperature,

and lead to the *assumption* of a rather complicated hydrogen bond system which is tentatively suggested by the chain lines inserted between atoms in Fig. II-21. Confirmation of this proposed hydrogen-bond system will have to await the results of neutron diffraction analyses. One short hydrogen bond, however, appears to be already established with certainty (H 4), and this is the bond between $O'_{III}(A)$ and $O'_{II}(A)$ in Fig. II-21 (bond length 2.44 Å).

In the configuration depicted in this figure, according to the formulation of Hoshino *et al.*, the proton is closer to the oxygen $O'_{III}(A)$ of the completely planar glycinium ion III. This is actually the reason *why* the group III is considered the glycinium ion, while the glycine group II is considered the zwitter-ion.

The molecular mechanism of polarization reversal in TGS is then described as follows (H 4). A reversal of the H association from group III to group II along the short $O'_{III}(A) - H - O'_{II}(A)$ bond involves a reversal of the former glycinium-glycine roles of these two groups: This means that group III becomes the zwitter-ion and group II becomes the glycinium ion. The $N_{II}(A)$ atom moves back into the plane of the remaining atoms, while the $N_{III}(A)$ atom moves away from its corresponding plane. These changes affect the position of the glycinium ion I via the complex hydrogen-bond system relating the nitrogens of the glycine groups with the oxygens of the sulfate groups. The coplanar glycinium ion I, inclined at 12.5° with respect to the plane at $b = 1/4$, flips over into the symmetrical position with respect to this same plane. As the nitrogen atom of this glycinium group lies about 0.5 Å away from the plane at $b = 1/4$, this would imply a remarkably large shift of the nitrogen (about 1 Å) along the direction of the monoclinic b axis. However, since the reported temperature factor of this atom is quite large (H 4) it is possible that an eventual interference between temperature factor and positional parameter would make the reported value of the latter rather inaccurate.

The importance of the role played by the glycine groups in the process of polarization onset and reversal is indirectly confirmed by the Raman investigations of TGS. The interpretation of the Raman spectra (T 5), (K 3) confirms the X-ray result that the SO_4 groups do not have tetrahedral symmetry at room temperature. The observed Raman lines also allow the conclusion that these groups maintain a mirror plane at room temperature. Thus, it follows that the SO_4 groups cannot bear an electric moment parallel to the twofold axis and the phenomenon of ferroelectricity must be attributed to the glycine groups (T 5).

The essential features of the molecular mechanisms proposed on the basis of the structural investigations appear, therefore, quite reasonable. No model theory has been developed, to date, on this ground.

Character of the Transition

A theoretical and experimental study of the characteristics of the ferroelectric transition in TGS has been carried out by Shibuya and Mitsui (S 3) through investigation of the diffuse X-ray scattering that is caused by disorder in the crystal. Both the dielectric data and the result of the structural analysis indicate that the ferroelectric transition in TGS (similarly to that in KH_2PO_4 and in Rochelle salt), is

and the intensity of the diffuse scattering by

$$I_c \propto B^2 \times \varepsilon.$$

It should be noted that, owing to the choice of the origin, B is not the imaginary part of the structure factor of the actual crystal but that of the basic structure and thus B has a finite value also above the Curie point. The direct proportionality of I_c with the dielectric constant predicts an anomaly of the diffuse scattering at the Curie point.

The experimental observations are in satisfactory agreement with these theoretical predictions (S 3). The observed diffuse scattering exhibits a pronounced peak at the Curie point. On the basis of these results, it can thus be confirmed that the ferroelectric phenomenon in TGS is due to a transition from a disordered to an ordered state.

10. Isomorphous Compounds

As mentioned in Section 1, two compounds isomorphous with TGS exhibit the same type of ferroelectric transition as TGS, viz. tri-glycine selenate (M 1) and tri-glycine fluoberyllate (P 1) Crystallographic data for these compounds were reported by Pepinsky *et al.* (P 1). The phenomenological behavior, so far as known, is similar in every respect to that of TGS (H 1) and the same holds, most probably, for the molecular mechanism involved. Table II-1 lists some of the pertinent data concerning TGS and its ferroelectric isomorphs. Pulsing experiments on the fluoberyllate have been carried out by Pulvari and Kuebler (*P* 3) and the effect of hydrostatic pressure on the selenate has been studied by Jona and Shirane (J 1). Mixed crystals of tri-glycine sulfate and selenate have been grown and investigated by Fatuzzo and Nitsche (F 4). The Curie temperature was found to vary linearly with composition, so that it is possible to prepare crystals having any desired Curie temperature in the range between 22° C and 49 °C. The dielectric properties of partially deuterated tri-glycine sulfate have been studied by Chapelle and Taurel (C 7).

TABLE II-1. DATA ON FERROELECTRIC TRI-GLYCINE SULFATE AND ISOMORPHS

Name of compound (Abbreviation) Chemical formula	Transition temperature (°C)	Spontaneous polarization P_s at T °C (C/cm^2)	ξ coefficient of free energy expansion (e.s.u./cm^2)$^{-2}$	Curie constant (°K)	Reference
Tri-glycine sulfate (TGS) $(NH_2CH_2COOH)_3 \cdot H_2SO_4$	49	2.8×10^{-6} at 20 °C	8.5×10^{-10}	3200	M 1, H 1, T 1
Tri-glycine selenate (TGSe) $(NH_2CH_2COOH)_3 \cdot H_2SeO_4$	22	3.2×10^{-6} at 0 °C	4.7×10^{-10}	4000	M 1, J 1
Tri-glycine fluoberyllate (TGFB) $(NH_2CH_2COOH)_3 \cdot H_2BeF_4$	70	3.2×10^{-6} at 20 °C	13.5×10^{-10}	2350	H 1

BIBLIOGRAPHY

(A 1) ABE, R., *J. Phys. Soc. Japan* **15**, 795 (1960).

(B 1) BURGESS, R. E., *Can. J. Phys.* **36**, 1569 (1958).

(C 1) CHYNOWETH, A. G., *Phys. Rev.* **113**, 159 (1959).
(C 2) CHYNOWETH, A. G. and ABEL, J. L., *J. Appl. Phys.* **30**, 1073 (1959).
(C 3) CHYNOWETH, A. G. and ABEL, J. L., *J. Appl. Phys.* **30**, 1615 (1959).
(C 4) CHYNOWETH, A. G., *Phys. Rev.* **117**, 1235 (1960).
(C 5) CHAPELLE, J. and TAUREL, L., *Compt. rend.* **249**, 378 (1959).
(C 6) CHYNOWETH, A. G. and FELDMAN, W. L., *J. Phys. Chem. Solids* **15**, 225 (1960).
(C 7) CHAPELLE, J. and TAUREL, L., *Compt. rend.* **249**, 1332 (1959).

(D 1) DOMANSKI, S., *Proc. Phys. Soc. (London)* **B 72**, 306 (1958).
(D 2) DROUGARD, M. E., LANDAUER, R. and YOUNG, D. R., *Phys. Rev.* **98**, 1010 (1955).
(D 3) DEVONSHIRE, A. F., Theory of Ferroelectrics, *Phil. Mag.* Suppl. **3**, 85, (1954).

(E 1) EHRENFEST, P., *Proc. Acad. Sci. Amsterdam* **36**, 153 (1933).
(E 2) EZHKOVA, Z. I., ZHDANOV, G. S. and UMANSKIJ, M. M., *Kristallografiya* **4**, 249 (1959).

(F 1) FATUZZO, E., *Helv. Phys. Acta* **31**, 309 (1958).
(F 2) FATUZZO, E. and MERZ, W. J., *Phys. Rev.* **116**, 61 (1959).
(F 3) FRÖHLICH, H., *Theory of Dielectrics*, ch. II, sec. 7, Oxford University Press, London (1958).
(F 4) FATUZZO, E. and NITSCHE, R., *Z. Elektrochem.* **63**, 970 (1959).
(F 5) FATUZZO, E., *Helv. Phys. Acta* **33**, 501 (1960).

(H 1) HOSHINO, S., MITSUI, T., JONA, F. and PEPINSKY, R., *Phys. Rev.* **107**, 1255 (1957).
(H 2) HOOTON, J. A. and MERZ, W. J., *Phys. Rev.* **98**, 409 (1955).
(H 3) HUSIMI, K. and KATAOKA, K., *J. Phys. Soc. Japan* **14**, 105 (1959).
(H 4) HOSHINO, S., OKAYA, Y. and PEPINSKY, R., *Phys. Rev.* **115**, 323 (1959).
(H 5) HALM, T. and BUERGER, M. J., *Z. Krist.* **108**, 419 (1957).

(J 1) JONA, F. and SHIRANE, G., *Phys. Rev.* **117**, 139 (1960).

(K 1) KONSTANTINOVA, V. P., SIL'VESTROVA, I. M. and ALEKSANDROV, K. S., *Kristallografiya* **4**, 69 (1959).
(K 2) KONSTANTINOVA, V. P., SIL'VESTROVA, I. M. and YURIN, V. A., *Kristallografiya* **4**, 125 (1959).
(K 3) KRISHNAN, R. S. and BALASUBRAMIAN, K., *Proc. Indian Acad. Sci.* **A 48**, 138 (1958).

(L 1) LURIO, A. and STERN, E., *J. Appl. Phys.* **31**, 1125 (1960).

(M 1) MATTHIAS, B. T., MILLER, C. E. and REMEIKA, J. P., *Phys. Rev.* **104**, 849 (1956).
(M 2) MERZ, W. J., *Phys. Rev.* **95**, 690 (1954).
(M 3) MARSH, R. E., *Acta Cryst.* **11**, 654 (1958).
(M 4) MILLER, R. C. and HEIDENREICH, R. D., *J. Appl. Phys.* **29**, 957 (1958).

(N 1) NITSCHE, R., *Helv. Phys. Acta* **31**, 306 (1958).
(N 2) NISHIOKA, A. and TAKEUCHI, M. *J., Phys. Soc. Japan* **14**, 971 (1959).
(N 3) NAKAMURA, E. and FURUICHI, J., *J. Phys. Soc. Japan* **15**, 2101 (1960).

(P 1) PEPINSKY, R., OKAYA, Y. and JONA, F., *Bull. Am. Phys. Soc.* **2**, No. 4, 220 (1957).
(P 2) PEARSON, G. L. and FELDMAN, W. L., *J. Phys. Chem. Solids* **9**, 28 (1959).
(P 3) PULVARI, C. F. and KUEBLER, W., *J. Appl. Phys.* **29**, 1742 (1958).

(S 1) SHUVALOV, L. A., ALEKSANDROV, K. S., and ZHELUDEV, I.S., *Kristallografiya* **4**, 130 (1959).
(S 2) SAVAGE, A. and MILLER, R. C., *J. Appl. Phys.* **30**, 1646 (1959).
(S 3) SHIBUYA, I. and MITSUI, T., *J. Phys. Soc. Japan* **16**, 479 (1961).

(T 1) TRIEBWASSER, S., *I.B.M.J. Research Developm.* **2**, 212 (1958).
(T 2) TAUREL, L., POUREL, E. and THOMASSIN, F., *Compt. rend.* **246**, 70 (1958).
(T 3) TOYODA, H., WAKU, S., SHIBATA, H. and TANAKA, Y., *J. Phys. Soc. Japan* **14**, 109 (1959).